Table S1 Site list

Table 1. Site characteristics including location, ecosystem type, climate, mean annual air temperature, annual sum of precipitation, leaf area index, and optimized parameters when monthly gross primary productivity (GPP) showed its maximum.

| Name | FLUXNET Short ID | AsiaFlux Short ID | Other Site Short ID | Country | Network | Location | Veg Type | C3/C4 | Köppen Climate | Annual Mean Temperature | Annual Sum Precipitation | LAI | Ω | $Vc_{max25}$ $\mu$ mol m$^{-2}$ s$^{-1}$ | $J_{max25}$ $\mu$ mol m$^{-2}$ s$^{-1}$ | $m_{bb}$ -- | Period | Reference |
|---|---|---|---|---|---|---|---|---|---|---|---|---|---|---|---|---|---|---|
| Chokurdakh | RU-Cok | - | | Russia | European FluxDB | 70°50'N 147°30'E | GRA | C3 | Dfc | -14.3 | 232 | 1.0 | 0.75 | 32.8 | 69.3 | 29.9 | 2003–2013 | van Huissleden et al. [2005] |
| Cherski | RU-Che | - | | Russia | European FluxDB | 68°37'N 161°20'E | WET | C3 | Dfc | -12.5 | 200 | N/A | 0.75 | 33.7 | 72.8 | 17.6 | 2002–2005 | Corradi et al. [2005] Merbold et al. [2009] |
| Pleistocene Park | - | - | AON | Russia | AON | 68°31'N 161°32'E | OSH | C3 | Dfc | -12.5 | 200 | N/A | 0.74 | 36.5 | 77.8 | 13.2 | 2009 2012–2014 | Euskirchen et al. [2017] |
| Seida/Vorkuta | RU-Vrt | - | | Russia | European FluxDB | 67°03'N 62°56'E | CSH | C3 | Dfc | -5.6 | 501 | 2.0 | 0.71 | 31.8 | 69.3 | 14.2 | 2008 | Marushchak et al. [2013] |
| Tura | RU-Tur | TUR | | Russia | AsiaFlux | 64°13'N 100°28'E | DNF | C3 | Dfc | -9.2 | 317 | 0.6 | 0.57 | 20.6 | 46.0 | 29.7 | 2004 | Nakai et al. [2008] |
| Nelegel | - | - | NEL | Russia | - | 62°19'N 129°30'E | DNF | C3 | Dfc | -9.5 | 238 | N/A | 0.57 | 9.4 | 18.7 | 47.0 | 2000–2006 | Machimura et al. [2005] |
| Siberia Yakutsk Larch Forest Site | RU-Skp | YLF | | Russia | AsiaFlux | 62°15'N 129°14'E | DNF | C3 | Dfc | -9.5 | 238 | 3.7 | 0.57 | 47.7 | 94.3 | 19.6 | 2003–2010 | Matsumoto et al. [2008] |
| Yakutsk Pine Forest Site | RU-Ylp | YPF | | Russia | AsiaFlux | 62°14'N 129°39'E | ENF | C3 | Dfc | -9.5 | 238 | 2.8 | 0.53 | 49.7 | 104.8 | 12.3 | 2004–2008 | Matsumoto et al. [2008] |
| Zotino | RU-Zot | - | | Russia | European FluxDB | 60°48'N 89°21'E | ENF | C3 | Dfc | -1.5 | 593 | 0.2 | 0.53 | 65.9 | 142.3 | 11.5 | 2002–2004 | Tanja et al. [2003] |
| Fyodorovskoye wet spruce stand | RU-Fyo | - | | Russia | European FluxDB | 56°28'N 32°55'E | ENF | C3 | Dfb | 3.9 | 711 | 3.5 | 0.53 | 127.1 | 266.9 | 11.1 | 1998–2014 | Milyukova et al. [2002] |
| Hakasia 5 yr | RU-Ha2 | - | | Russia | European FluxDB | 54°46'N 89°57'E | GRA | C3 | Dfc | 0.4 | 304 | N/A | 0.75 | 58.3 | 120.8 | 7.5 | 2002–2003 | Belelli Marchesini [2007] |
| Hakasia Steppe | RU-Ha1 | - | | Russia | European FluxDB | 54°44'N 90°00'E | GRA | C3 | Dfc | 0.4 | 304 | N/A | 0.75 | 40.2 | 81.6 | 7.5 | 2002–2004 | Belelli Marchesini et al. [2007] |
| Hakasia 10 yr | RU-Ha3 | - | | Russia | European FluxDB | 54°42'N 89°05'E | GRA | C3 | Dfc | 0.4 | 304 | N/A | 0.75 | 36.0 | 75.2 | 13.8 | 2004–2004 | Belelli Marchesini [2007] |
| Southern Khentei Taiga | MN-Knt | SKT | | Mongolia | AsiaFlux | 48°21'N 108°39'E | DNF | C3 | Dwb | -2.9 | 282 | 4.4 | 0.57 | 141.9 | 258.5 | 8.8 | 2003–2006 | Li et al. [2005b] |
| Kherlenbayan Ulaan | MN-Knr | KBU | | Mongolia | AsiaFlux | 47°13'N 108°44'E | GRA | C3/C4 | BSk | 1.2 | 196 | 0.6 | 0.75 | 33.6 | 66.0 | 15.9 | 2003–2008 | Li et al. [2005a] |
| Laoshan | CN-Lao | LSH | | China | AsiaFlux | 45°17'N 127°35'E | DNF | C3 | Dwb | 2.8 | 724 | 2.5 | 0.57 | 163.0 | 314.4 | 8.4 | 2002–2006 | Wang et al. [2005] |
| Teshio CC-LaG experiment site | JP-Tef | TSE | | Japan | AsiaFlux | 45°03'N 142°06'E | MF | C3 | Dfb | 5.7 | 1000 | 3.2 | 0.69 | 141.9 | 281.9 | 8.5 | 2002 | Takagi et al. [2009] |
| | | | | | | | CSH (clear cut) | C3 | Dfb | 5.7 | 1000 | 9.1 | 0.71 | 64.0 | 135.5 | 11.5 | 2004–2012 | Takagi et al. [2009] |
| Moshiri Birch Forest Site | JP-MBF | MBF | | Japan | AsiaFlux | 44°23'N 142°19'E | DBF | C3 | Dfb | 6.7 | 1184 | 2.7 | 0.70 | 95.1 | 197.9 | 15.7 | 2003–2005 | Matsumoto et al. [2008] |
| Moshiri Mixed Forest Site | JP-MMF | MMF | | Japan | AsiaFlux | 44°20'N 142°15'E | MF | C3 | Dfb | 6.7 | 1184 | 3.4 | 0.69 | 134.2 | 282.1 | 11.1 | 2003–2005 | Matsumoto et al. [2008] |
| Sapporo | JP-Sap | SAP | | Japan | FFPRI | 42°59'N 141°23'E | DBF | C3 | Dfb | 7.2 | 933 | 4.0 | 0.70 | 111.9 | 224.9 | 14.0 | 2000–2004 | Kitamura et al. [2012] |
| Inner Mongolia Light Grazing | | MLG | | Mongolia | NIAES | 42°58'N 120°43'E | GRA | C3/C4 | Bsk | N/A | N/A | N/A | 0.75 | 14.8 | 29.9 | 27.2 | 1993-1994 | Harazono et al. [1993] Miyata et al. [1993] |
| Inner Mongolia Medium Grazing | | MMG | | Mongolia | NIAES | 42°58'N 120°43'E | GRA | C3/C4 | Bsk | N/A | N/A | N/A | 0.75 | 18.7 | 45.7 | 3.8 | 1994 | Harazono et al. [1993] Miyata et al. [1993] |
| Inner Mongolia Soybean | | MSB | | Mongolia | NIAES | 42°58'N 120°43'E | CRO | C3/C4 | Bsk | N/A | N/A | N/A | 0.75 | 27.9 | 66.7 | 13.0 | 1993 | Harazono et al. [1993] Miyata et al. [1993] |

| | | | | | | | | | | | | | | | | | |
|---|---|---|---|---|---|---|---|---|---|---|---|---|---|---|---|---|---|
| Tomakomai Flux Research Site | JP-Tom | TMK | Japan | AsiaFlux | 42°44'N 141°31'E | DNF | C3 | Dfb | 6.20 | 1043.00 | 9.20 | 0.57 | 292.3 | 658.3 | 14.4 | 2001–2003 | Hirata et al. [2007] |
| Changbaishan | CH-Cha | CBS | China | AsiaFlux | 42°24'N 128°50'E | MF | C3 | Dwb | 3.60 | 713.00 | 4.50 | 0.69 | 89.4 | 177.7 | 14.0 | 2003–2005 | Yu et al. [2006, 2008] |
| Appi | JP-App | API | Japan | FFPRI | 40°00'N 140°56'E | DBF | C3 | Dfa | 6.10 | 1869.00 | 4.80 | 0.70 | 149.0 | 314.5 | 10.5*1 | 2000–2006 | Yasuda et al. [2012] |
| KoFlux Seolmacheon Site | KR-Seo | SMK | Korea | AsiaFlux | 37°56'N 126°57'E | MF | C3 | Dwa | 13.43 | 1485.90 | N/A | 0.69 | 37.6 | 77.9 | 28.4 | 2008 | Kwon et al. [2009] |
| KoFlux Gwangneung Deciduous forest | KR-Kw2 | GDK | Korea | AsiaFlux | 37°45'N 127°09'E | MF | C3 | Dwa | 11.50 | 1332.00 | 6.00 | 0.69 | 67.0 | 122.6 | 7.8 | 2006–2014 | Kwon et al. [2009] |
| KoFlux Gwangneung Coniferous forest | KR-Kw1 | GCK | Korea | AsiaFlux | 37°45'N 127°10'E | ENF | C3 | Dwa | 11.50 | 1332.00 | 8.00 | 0.53 | 68.7 | 126.4 | 9.7 | 2007–2014 | Kwon et al. [2010] |
| Tibet | CN-Ha2 | HBG | China | AsiaFlux | 37°40'N 101°20'E | OSH | C3 | Dwb | -1.70 | 600.00 | 2.80 | 0.74 | 78.5 | 157.3 | 5.8 | 2003–2004 | Yu et al. [2006] |
| Qinghai Flux Research Site | - | QHB | China | AsiaFlux | 37°36'N 101°20'E | GRA | C3 | BS | 13.10 | 528.00 | 6.00 | 1.00 | 105.6 | 200.0 | 4.6 | 2002–2004 | Kato et al. [2006] |
| Yucheng | CN-Yuc | YCS | China | AsiaFlux | 36°57'N 116°36'E | CRO | C3/C4 | Dwa | 13.10 | 528.00 | 6.00 | 0.75 | 126.3 | 267.4 | 20.6 | 2003–2005 | Yu et al. [2006] |
| Takayama deciduous broadleaf forest site | JP-Tak | TKY | Japan | AsiaFlux | 36°09'N 137°25'E | DBF | C3 | Dfb | 6.50 | 2275.00 | 4.00 | 0.70 | 135.5 | 300.0 | 7.9 | 1999–2007 | Saigusa et al. [2005] |
| Takayama evergreen coniferous forest site | JP-Ta2 | TKC | Japan | AsiaFlux | 36°08'N 137°22'E | ENF | C3 | Dfb | 10.70 | 1722.00 | 5.20 | 0.53 | 163.7 | 321.5 | 7.3 | 2006–2010 | Saitoh et al. [2010] |
| Mase paddy flux site | JP-Mas | MSE | Japan | AsiaFlux | 36°04'N 140°01'E | CRO | C3 | Cfa | 13.70 | 1200.00 | 5.00 | 1.00 | 125.0 | 232.3 | 10.2 | 2001–2006 | Saito et al. [2005] |
| Yawara rice paddy | | YRP | Japan | NIAES | 36°00'N 140°01'E | CRO | C3 | Cfa | 13.7 | 1200 | 2.2 | 1.00 | 108.1 | 192.2 | 18.8 | 1993-1995 | |
| NIAES soybean | | NSB | Japan | NIAES | 36°01'N 140°07'E | CRO | C3 | Cfa | 13.7 | 1200 | N/A | 0.75 | 66.3 | 135.5 | 17.5 | 1990 | Harazono et al. [1996] |
| Lotus paddy | | NLP | Japan | NIAES | 36°05' N 140° 15'E | CRO | C3 | Cfa | 14.4 | 1187.8 | 3.5 | 0.75 | 100.4 | 189.2 | 8.8 | 1997 | Takagi et al. [2003] |
| Kawagoe | | KWG | Japan | FFPRI | 35°52'N 139°29'E | DBF | C3 | Cfa | 15.2 | 1569 | 5.5 | 0.70 | 94.3 | 179.3 | 10.5*1 | 1997-2002 | Yasuda et al. [2001] |
| Fujiyoshida | JP-Fuj | FJY | Japan | FFPRI | 35°27'N 138°46'E | ENF | C3 | Cfb | 10.1 | 1483 | 4.4 | 0.53 | 111.0 | 211.7 | 7.9 | 2000–2008 | Mizoguchi et al. [2012] |
| Fuji Hokuroku | JP-FHK | FHK | Japan | AsiaFlux | 35°27'N 138°46'E | DNF | C3 | Cfb | 9.6 | 1566 | 5.0 | 0.57 | 173.5 | 382.3 | 11.0 | 2006–2013 | Takahashi et al. [2015] |

| | | | | | | | | | | | | | | | | | | |
|---|---|---|---|---|---|---|---|---|---|---|---|---|---|---|---|---|---|---|
| Seto Mixed Forest Site | JP-SMF | SMF | | Japan | AsiaFlux | 35°16'N 137°05'E | MF | C3 | Cfa | 13.4 | 1486 | N/A | 0.69 | 115.1 | 225.8 | 10.3 | 2002–2011 | Matsumoto et al. [2008] |
| Kiryu Experimental Watershed | JP-KEW | KEW | | Japan | AsiaFlux | 34°58'N 136°00'E | ENF | C3 | Cfa | 13.6 | 1645 | 5.5 | 0.53 | 136.5 | 309.7 | 8.3 | 2001–2007 | Kosugi et al. [2013] |
| Akou green belt | | AKO | | Japan | AsiaFlux | 34º 44'N 134º 22' E | EBF | C3 | Cfa | 15.2 | 1159 | 5.0 | 0.66 | 37.0 | 77.4 | 12.8 | 2000-2003 | Kosugi et sl. [2005] |
| KoFlux Haenam Site | KR-Hae | HFK | | Korea | AsiaFlux | 34°33'N 126°34'E | CRO | C3 | Cfa | 13.3 | 1306 | 3.5 | 0.75 | 75.2 | 143.2 | 19.4 | 2003–2006 2008-2013 | Kwon et al. [2010] |
| Kahoku | JP-Kah | KHW | | Japan | FFPRI | 33°08'N 130°43'E | ENF | C3 | Cfa | 15.1 | 2106 | 5.2 | 0.53 | 50.8 | 101.8 | 8.3[*1] | 2000–2003 | Shimizu et al. [1999] |
| Yatir | IL-Yat | - | | Israel | European FluxDB | 31°21'N 35°03'E | ENF | C3 | BS | 22 | 275 | 1.5 | 0.53 | 49.5 | 110.2 | 18.2 | 2001–2009 | Sprintsin et al. [2011] |
| Qianyanzhou | CN-Qia | QYZ | | China | AsiaFlux | 26°44'N 115°04'E | ENF | C3 | Cfa | 18.6 | 1488.9 | 3.6 | 0.53 | 32.5 | 66.7 | 20.2 | 2003–2004 | Yu et al. [2006] |
| Chi-Lan Mountain Research Site | TW-Chn | CLM | | Taiwan | AsiaFlux | 24°35'N 121°25'E | ENF | C3 | Cfa | 13 | 4000 | 6.1 | 0.53 | 74.1 | 162.3 | 11.9 | 2007–2009 | Hsieh et al. [2008] |
| Xishungbanna | CN-Xsh | BNS | | China | AsiaFlux | 21°57'N 101°12'E | EBF | C3 | Am | 21 | 1492 | 6.2 | 0.66 | 45.8 | 91.9 | 9.7 | 2003–2005 | Tan et al. [2011] |
| Mae Klong | TH-Mae | MKL | | Thailand | AsiaFlux | 14°35'N 98°51'E | EBF | C3 | Am | 25 | 1500 | 3.0 | 0.70 | 336.8 | 822.9 | 4.7 | 2003–2004 | Gamo et al. [2005] |
| Sakaerat | TH-Sak | SKR | | Thailand | AsiaFlux | 14°30'N 101°55'E | EBF | C3 | Aw | 24 | 1250 | 4.0 | 0.66 | 247.2 | 486.3 | 7.0 | 2001–2003 | Gamo et al. [2005] |
| IRRI Flux Research Site | PH-Rin | IRI-NFL | | Philippines | AsiaFlux | 14°09'N 121°16'E | CRO | C3 | Am | 27.5 | 2075 | 6.0 | 1.00 | 54.2 | 101.0 | 14.6 | 2009–2010 | Alberto et al. [2009] |
| IRRI Flux Research Site | PH-Rif | IRI-FL | | Philippines | AsiaFlux | 14°08'N 121°15'E | CRO | C3 | Am | 27.5 | 2075 | 7.4 | 1.00 | 100.2 | 193.5 | 11.3 | 2009–2010 2013-2014 | Alberto et al. [2009] |
| Lambir Hills National Park | | LHP | | Malaysia | AsiaFlux | 4°12'N 114°02'E | EBF | C3 | Af | 27 | 2740 | 6.2 | 0.66 | 90.6 | 190.8 | 10.0 | 2001-2002 | Kumagai et al. [2006] |
| Pasoh Forest Reserve | MY-PSO | PSO | | Malaysia | AsiaFlux | 2°58'N 102°18'E | EBF | C3 | Af | 25.3 | 1865 | 6.5 | 0.66 | 106.4 | 202.6 | 16.1 | 2003–2009 | Kosugi et al. [2008] |
| Palangkaraya Peat Swamp Forest with little drainage | - | -- | PUF | Indonesia | - | 2°19'S 113°00'E | EBF | C3 | Af | 26.3 | 2231 | 5.0 | 0.66 | 112.8 | 218.4 | 18.6 | 2004–2008 | Hirano et al. [2012] |
| Palangkaraya drained burnt ex - Peat Swamp Forest | - | -- | PDB | Indonesia | - | 2°20'S 114°02'E | CSH (Burn) | C3 | Af | 26.3 | 2231 | 2.4 | 0.75 | 29.6 | 59.5 | 22.0 | 2004–2009 | Hirano et al. [2012] |
| Palangkaraya drained Forest | ID-Pal | PDF | | Indonesia | AsiaFlux | 2°21'S 114°02'E | EBF | C3 | Af | 26.3 | 2231 | 5.6 | 0.66 | 112.3 | 233.0 | 15.0 | 2001–2008 | Hirano et al. [2007] |
| Sodankyla | FI-Sod | | | Finland | FLUXNET 2015 | 67°58'N 24°14'W | ENF | C3 | Unknown | -1.0 | 500 | 1.2 | 0.53 | 61.3 | 131.7 | 16.1 | 2002-2014 | Rinne et al. [2000] |
| Hyytiala | FI-Hyy | | | Finland | FLUXNET 2015 | 61°50'N 2°17'W | ENF | C3 | Unknown | 3.8 | 709 | 6.7 | 0.53 | 83.2 | 169.6 | 19.2 | 1997-2011 | Kolari et al. [2007] |
| Manitoba NOBS | CA-Man | | | Canada | FLUXNET 2015 | 55°52'N -98°29'W | ENF | C3 | Dfc | -3.2 | 520 | 4.2 | 0.53 | 37.6 | 78.2 | 17.2 | 1994-2008 | Dunn et al. [2007] |
| Soroe | DK-Sor | | | Denmark | FLUXNET 2015 | 55°9'N 5°44'W | DBF | C3 | Unknown | 8.2 | 660 | 5.0 | 0.70 | 212.6 | 496.7 | 18.3 | 2003-2013 | Pilegaard et al. [2001] |
| Loobos | NL-Loo | | | Netherlands | FLUXNET 2015 | 52°18'N 4°31'W | ENF | C3 | Unknown | 9.8 | 786 | 2.0 | 0.53 | 103.2 | 227.2 | 14.0 | 1996-2013 | Dolman et al. [2002] |
| Brasschaat | BE-Bra | | | Belgique | FLUXNET 2015 | 51°18'N 4°31'W | MF | C3 | Unknown | 9.8 | 750 | 3.6 | 0.69 | 84.2 | 173.2 | 13.1 | 1999-2014 | Carrara et al. [2003] |
| Gebesee | DE-Geb | | | Germany | FLUXNET 2015 | 51°6'N 10°54'W | CRO | C3 | Unknown | 8.5 | 470 | 4.0 | 0.75 | 144.3 | 310.2 | 18.6 | 2001-2014 | Anthoni et al. [2004] |
| Hainich | DE-Hai | | | Germany | FLUXNET 2015 | 51°4'N 10°27'W | DBF | C3 | Unknown | 8.3 | 720 | 6.1 | 0.70 | 142.7 | 326.4 | 16.7 | 2000-2009 | Anthoni et al. [2004] |
| Tharandt | DE-Tha | | | Germany | FLUXNET 2015 | 50°57'N 13°33'W | ENF | C3 | Cfb | 7.7 | 820 | 7.6 | 0.53 | 135.3 | 313.7 | 11.5 | 1996-2014 | Grünwald and Berhofer [2007] |
| Grillenburg | DE-Gri | | | Germany | FLUXNET 2015 | 50°57'N 13°30'W | GRA | C3 | Cfb | 7.2 | 853 | 7.6 | 0.75 | 105.6 | 223.0 | 14.5 | 2004-2014 | Prescher et al. [2010] |
| Klingenberg | DE-Kli | | | Germany | FLUXNET 2015 | 50°53'N 13°31'W | CRO | C3/C4 | Cfb | 9.0 | 750 | 9.7 | 0.75 | 200.4 | 429.1 | 12.8 | 2004-2014 | Prescher et al. [2010] |

| | | | | | | | | | | | | | | | | |
|---|---|---|---|---|---|---|---|---|---|---|---|---|---|---|---|---|
| Lonzee | BE-Lon | Belgique | FLUXNET 2015 | 50°33'N 4°44'W | CRO | C3 | Cfb | 10.0 | 800 | 4.5 | 0.75 | 192.8 | 438.6 | 15.3 | 2004-2014 | Moureaux et al. [2006] |
| Neustift | AT-Neu | Austria | FLUXNET 2015 | 47°7'N 11°19'W | GRA | C3 | Unknown | 6.3 | 852 | 6.5 | 0.75 | 267.6 | 619.6 | 10.4 | 2002–2012 | Wohlfahrt et al. [2008] |
| Fruebuel | CH-Fru | Switzerland | FLUXNET 2015 | 47°6'N 8°32'W | GRA | C3 | Unknown | 7.2 | 1651 | 4.0 | 0.75 | 177.0 | 371.9 | 10.6 | 2005-2012 | Zeeman et al. [2010] |
| Davos | CH-Dav | Switzerland | FLUXNET 2015 | 46°48'N 9°51'W | ENF | C3 | Unknown | 2.8 | 1062 | 3.9 | 0.53 | 90.3 | 199.0 | 14.2 | 1997-2011 | Zweife et al. [2010] |
| Renon | IT-Ren | Italy | FLUXNET 2015 | 46°35'N 11°26'W | ENF | C3 | Unknown | 4.7 | 809 | 5.1 | 0.53 | 106.5 | 223.6 | 15.7 | 2002-2012 | Montagnani et al. [2009] |
| Sylvania Wilderness Area | US-Syv | USA | FLUXNET 2015 | 46°14'N -89°20'W | MF | C3 | Dfb | 3.8 | 826 | 7.5 | 0.69 | 101.9 | 229.8 | 13.0 | 2001-2014 | Desai et ak. [2005] |
| Lost Creek | US-Los | USA | FLUXNET 2015 | 46°4'N -89°58'W | WET | C3 | Dfb | 4.1 | 828 | 4.9 | 0.75 | 88.2 | 169.7 | 13.2 | 2001-2014 | Sulman et al. [2009] |
| Monte Bondone | IT-MBo | Italy | FLUXNET 2015 | 46°0'N 11°2'W | GRA | C3 | Unknown | 5.1 | 1214 | 2.9 | 0.75 | 150.5 | 322.6 | 14.5 | 2003-2014 | Marcolla & Cescatti [2005] |
| Lavarone | IT-Lav | Italy | FLUXNET 2015 | 45°57'N 11°16'W | ENF | C3 | Unknown | 7.8 | 1291 | 8.0 | 0.53 | 176.0 | 363.1 | 9.5 | 2003-2014 | Cescatti & Marcolla [2004] |
| Willow Creek | US-WCr | USA | FLUXNET 2015 | 45°48'N -90°4'W | DBF | C3 | Dfb | 4.0 | 787 | 5.4 | 0.70 | 104.2 | 220.8 | 23.3 | 1999-2014 | Cook et al. [2004] |
| Univ. of Mich. Biological Station | US-UMB | USA | FLUXNET 2015 | 45°33'N -84°42'W | DBF | C3 | Dfb | 5.8 | 803 | 3.5 | 0.70 | 108.2 | 226.5 | 16.2 | 2000-2014 | Goucgh et al. [2013] |
| Le Bray | FR-LBr | France | FLUXNET 2015 | 44°43'N -0°46'W | ENF | C3 | Unknown | 13.6 | 900 | 3.5 | 0.53 | 88.1 | 185.1 | 17.0 | 1996-2008 | Berbigier et al. [2001] |
| Metolius mature ponderosa pine | US-Me2 | USA | FLUXNET 2015 | 44°27'N -121°33'W | ENF | C3 | Csb | 6.3 | 523 | 3.7 | 0.53 | 105.0 | 224.0 | 19.7 | 2002-2014 | Sun et al. [204] |
| Puechabon | FR-Pue | France | FLUXNET 2015 | 43°44'N 3°36'W | EBF | C3 | Unknown | 13.5 | 883 | 2.9 | 0.66 | 61.3 | 122.8 | 17.6 | 2001-2014 | Rambal et al. [2003] |
| Sam Rossore | IT-SRo | Italy | FLUXNET 2015 | 43°43'N 10°17'W | ENF | C3 | Unknown | 14.2 | 920 | 4.2 | 0.53 | 92.1 | 196.7 | 22.3 | 2000-2008 | Chiesa et al [2005] |
| Harvard Forest | US-Ha1 | USA | FLUXNET 2015 | 42°32'N 72°10'W | DBF | C3 | Dfb | 6.6 | 1071 | 5.5 | 0.70 | 143.9 | 305.0 | 13.0 | 1992-2012 | Urbanski et al. [2007] |
| Collelongo | IT-Col | Italy | FLUXNET 2015 | 41°50'N 13°35'W | DBF | C3 | Unknown | 6.3 | 1180 | 6.8 | 0.70 | 138.9 | 285.1 | 8.8 | 1996-2014 | Scartazza et al. [2004] |
| Castelpoiziano | IT-Cpz | Italy | FLUXNET 2015 | 41°42'N 12°18'W | EBF | C3 | Unknown | 15.6 | 780 | 3.5 | 0.66 | 97.5 | 193.5 | 15.3 | 2000-2008 | Garbulsky et al. [2008] |
| Niwot Ridge Forest (LTER NWT1) | US-NR1 | USA | FLUXNET 2015 | 40°1'N 105°32'W | ENF | C3 | Dfc | 1.5 | 800 | 5.6 | 0.53 | 80.9 | 168.3 | 15.5 | 1999-2014 | Monson et al. [2002] |
| Morgan Monroe State Forest | US-MMS | USA | FLUXNET 2015 | 39°19'N 86°25'W | DBF | C3 | Cfa | 10.9 | 1032 | 4.7 | 0.70 | 129.3 | 260.7 | 15.2 | 1999-2014 | Oliphant et al. [2004] |
| Tonzi Ranch | US-Ton | USA | FLUXNET 2015 | 38°24'N 120°57'W | WSA | C3 | Csa | 15.8 | 559 | 0.7 | 0.74 | 69.1 | 145.7 | 12.0 | 2001-2014 | Baldocchi et al. [2010] |
| Vaira Ranch-Ione | US-Var | USA | FLUXNET 2015 | 38°24'N 120°57'W | GRA | C3 | Csa | 15.8 | 559 | 2.8 | 0.75 | 82.3 | 180.7 | 16.6 | 2000-2014 | Ma et al. [2007] |
| Santa Rita mesquite savanna | US-SRM | USA | FLUXNET 2015 | 31°49'N 110°52'W | WSA | C3/C4 | Bsk | 17.9 | 380 | 0.4 | 0.74 | 48.2 | 101.1 | 13.6 | 2004-2014 | Scott et al. [2009] |
| Wahut Gulch Kendall Grassland | US-Wkg | USA | FLUXNET 2015 | 31°44'N 109°56'W | GRA | C3/C4 | Bsk | 15.6 | 407 | 1.0 | 0.75 | 35.0 | 72.5 | 11.3 | 2004-2014 | Scott et al. [2010] |
| Howard Springs | AU-How | Australia | FLUXNET 2015 | 12°17'S 131°05'E | WSA | C3 | Aw | 27.0 | 1449 | 2.3 | 0.74 | 85.6 | 183.9 | 12.2 | 2001–2014 | Hutley et al. [2005] |
| Tumbarumba | AU-Tum | Australia | FLUXNET 2015 | 35°39'S 148°09'E | EBF | C3 | Cfb | 10.7 | 1159 | 2.4 | 0.66 | 262.9 | 535.5 | 11.1 | 2001–2014 | Leuning et all. [2005] |
| Demokeya | SD-DEM | Sudan | FLUXNET 2015 | 13°17'N 30°28'E | WSA | C3/C4 | Bw | 26.0 | 320 | 1.00 | 0.74 | 43.8 | 90.3 | 10.2 | 2007–2009 | Ardö et al. [2008] |
| Santarem-Km83-L | BR-Sa3 | Brazil | FLUXNET 2015 | 3°1'S 54°58'W | EBF | C3 | Am | 26.12 | 2044 | N/A | 0.66 | 64.2 | 134.4 | 27.0 | 2000–2003 | Goulden et al. [2006] |
| Guyaflux | GF-Guy | French Guyai | FLUXNET 2015 | 5°17'S 52°55'E | EBF | C3 | Am | 25.7 | 3041 | 7.0 | 0.66 | 115.2 | 227.7 | 19.2 | 2004–2014 | Bonal et al. [2008] |
| Mongu | ZM-Mon | Zambia | FLUXNET 2015 | 15°26'S 23°15'E | DBF | C3 | Am | 25.0 | 945 | 1.6 | 0.70 | 74.1 | 163.0 | 12.0 | 2007–2009 | Merbold et al. [2009] |

| | | | | | | | | | | | | | | | | |
|---|---|---|---|---|---|---|---|---|---|---|---|---|---|---|---|---|
| Skukuza | ZA-KRU | South Africa | FLUXNET 2015 | 25°1'S 31°30'E | WSA | C3/C4 | Cwa | 21.9 | 359 | N/A | 0.74 | 63.4 | 124.7 | 10.5 | 2000–2010 | Kutsch et al. [2008] |
| Virasoro | AR-Vir | Argentina | FLUXNET 2015 | 28°14'S 56°11'W | ENF | C3 | Csb | 21.10 | 1800.00 | N/A | 0.53 | 152.0 | 330.5 | 7.8 | 2010–2012 | Posse et al. [2016] |
| San Luis | AR-SLu | Argentina | FLUXNET 2015 | 33°28'S 66°28'W | MF | C3 | Bwk | 19.69 | 4000 | N/A | 0.69 | 178.3 | 358.3 | 17.3 | 2009–2011 | Ulke et al. [2015] |

*1 Evapotranspiration was not provided by the database. The value of $m_{bb}$ was used from same vegetation type in Japan for simulating evapotranspiration.

Table S2. Sensitivity analysis for estimating how the eddy covariance data constrained the $CO_2$ fertilization effect for gross primary productivity (GPP), canopy-integrated stomatal conductance (gs), and intrinsic water use efficiency (iWUE). Range of uncertainties were estimated with simulations by input biased parameters ($Vc_{max25}$, $J_{max25}$, and $m_{bb}$). We added or subtracted 1σ of parameter-variations within the plant functional type to the optimized parameters, and then estimated the range of uncertainties for non-constrained simulation. This test assumed that arbitrarily chosen parameters were distributed within these variations.

| | | Relative change | | Best parameters | | | parameter +1σ | | | parameter -1σ | | | range of uncertainties | | |
|---|---|---|---|---|---|---|---|---|---|---|---|---|---|---|---|
| Site | PFT | Vcmax | m | GPP | gs | iWUE | GPP | gs | iWUE | GPP | gs | iWUE | GPP | gs | iWUE |
| -- | -- | % | % | % $ppm^{-1}$ | % $ppm^{-1}$ | % $ppm^{-1}$ | % $ppm^{-1}$ | % $ppm^{-1}$ | % $ppm^{-1}$ | % $ppm^{-1}$ | % $ppm^{-1}$ | % $ppm^{-1}$ | % | % | % |
| AU-How | WSA | 28 | 7 | 0.16 | -0.06 | 0.22 | 0.15 | -0.07 | 0.22 | 0.17 | -0.05 | 0.22 | 10 | 25 | 1 |
| AU-Tum | EBF | 72 | 36 | 0.12 | -0.09 | 0.20 | 0.10 | -0.11 | 0.20 | 0.16 | -0.04 | 0.20 | 54 | 78 | 0 |
| Ca-Man | ENF | 42 | 31 | 0.16 | -0.08 | 0.24 | 0.15 | -0.09 | 0.24 | 0.18 | -0.05 | 0.23 | 17 | 50 | 4 |
| DE-Geb | CRO | 47 | 26 | 0.15 | -0.06 | 0.20 | 0.13 | -0.06 | 0.19 | 0.16 | -0.05 | 0.21 | 19 | 14 | 10 |
| DE-Sor | DBF | 25 | 30 | 0.09 | -0.11 | 0.19 | 0.08 | -0.11 | 0.18 | 0.10 | -0.10 | 0.20 | 25 | 10 | 7 |
| FI-Hyy | ENF | 42 | 31 | 0.15 | -0.09 | 0.23 | 0.12 | -0.11 | 0.22 | 0.16 | -0.07 | 0.23 | 27 | 39 | 2 |
| FI-Sod | ENF | 42 | 31 | 0.16 | -0.07 | 0.22 | 0.14 | -0.09 | 0.22 | 0.17 | -0.05 | 0.21 | 19 | 63 | 5 |
| FR-LBr | ENF | 42 | 31 | 0.13 | -0.10 | 0.23 | 0.12 | -0.11 | 0.23 | 0.16 | -0.08 | 0.23 | 29 | 34 | 3 |
| FR-Pue | EBF | 72 | 36 | 0.15 | -0.07 | 0.22 | 0.14 | -0.09 | 0.22 | 0.16 | -0.03 | 0.19 | 16 | 79 | 13 |
| IT-MBo | GRA | 88 | 56 | 0.16 | -0.05 | 0.21 | 0.13 | -0.05 | 0.18 | 0.19 | -0.02 | 0.20 | 35 | 65 | 11 |
| US-Ha1 | DBF | 25 | 30 | 0.14 | -0.09 | 0.23 | 0.13 | -0.10 | 0.23 | 0.16 | -0.07 | 0.23 | 23 | 40 | 1 |
| US-Los | WET | 63 | 20 | 0.14 | -0.07 | 0.21 | 0.13 | -0.08 | 0.21 | 0.17 | -0.04 | 0.21 | 30 | 56 | 2 |
| US-Ton | WSA | 28 | 7 | 0.15 | -0.05 | 0.19 | 0.14 | -0.06 | 0.19 | 0.15 | -0.05 | 0.19 | 8 | 23 | 0 |
| US-UMB | DBF | 25 | 30 | 0.12 | -0.10 | 0.21 | 0.12 | -0.10 | 0.21 | 0.13 | -0.08 | 0.21 | 15 | 15 | 2 |

Table S3. List of models, parameters that were estimated using a multiple constraint, and methods for estimating model parameters.

| Model | Parameter | Constraint | Method |
|---|---|---|---|
| Biochemical photosynthesis model (Farquhar et al., 1980; Eq. A1) | $Vc_{max25}$, $J_{max25}$ | GPP, PPFD, $[CO_2]$, Leaf area index Leaf temperature, Stomatal conductance | Mathematical optimization using SCE-UA method |
| Stomatal conductance model (Ball et al., 1987; A22) | $m_{bb}$, $b_{bb}$ | Water vapor flux, GPP, $g_b$, Specific humidity, Leaf temperature, $[CO_2]$ | Mathematical optimization using SCE-UA method |
| Bulk model (Eq. A29, A31) | $g_b$, Leaf temperature | Friction velocity, Wind speed, Sensible heat flux, Air temperature, Barometric pressure, Leaf area index | Inverse estimate of the bulk equation |

$Vc_{max25}$ : maximum carboxylation rate at 25 $^{o}$C
$J_{max25}$ : maximum electron transport rate at 25 $^{o}$C
$m_{bb}$ : stomatal conductance parameters
$b_{bb}$ : stomatal conductance parameters
$g_b$ : aerodynamic conductance of sensible heat

GPP : Gross Primary Productivity
PPFD : Photosynthetically Photon Flux Density
$[CO_2]$ : atmospheric $CO_2$ concentration

Table S4. Global trends in gross primary productivity (GPP) and evapotranspiration (ET) reprocessed using MODIS collection 6 data after Kondo et al., (2015), fluxes subtracting the $CO_2$ fertilization effect, and the CO2 fertilization effect by different input data in the upscaling. The trends using the different inputs of 1) combinations of CRU-TS climate data and National Centers for Environmental Prediction (NCEP) / the National Center for Atmospheric Research (NCAR) reanalysis (CRU/NCEP) data with MOD15 LAI data, 2) combinations of ERA5 climate data with MOD15 LAI data, and 3) combinations of CRU/NCEP climate data with the Global Inventory Modeling and Mapping Studies (GIMMS) LAI3g product (Zhu et al., 2013) are compared.

| Data | GPP trend | GPP trend without the $CO_2$ fertilization | $CO_2$ fertilization in GPP | ET trend | ET trend without the $CO_2$ fertilization | $CO_2$ fertilization in ET |
|---|---|---|---|---|---|---|
| | g C $m^{-2}$ $yr^{-2}$ | g C $m^{-2}$ $yr^{-2}$ | g C $m^{-2}$ $yr^{-2}$ | mm $yr^{-2}$ | mm $yr^{-2}$ | mm $yr^{-2}$ |
| CRU/NCEP + MOD15 | 2.6065 | 0.9807 | 1.6258 | 1.0363 | 1.2437 | -0.2074 |
| ERA5 + MOD15 | -- | 0.9827 | 1.6238 | -- | 1.2437 | -0.2074 |
| CRU/NCEP + LAI3g | -- | 0.9810 | 1.6255 | -- | 1.2418 | -0.2055 |

# Figure S1

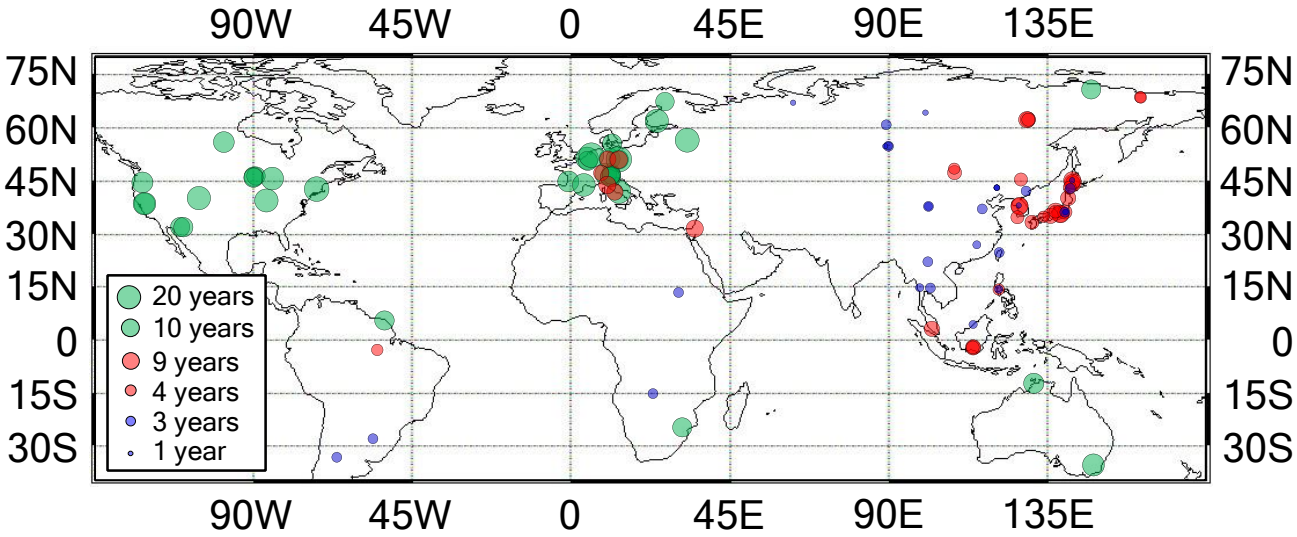


Spatial distributions of eddy covariance towers used in this study (Table S1). Size and colors of the circles represent the number of years available for the analysis; data containing one to three years (blue), four to nine years (red), and ten or more years (green).

Figure S2

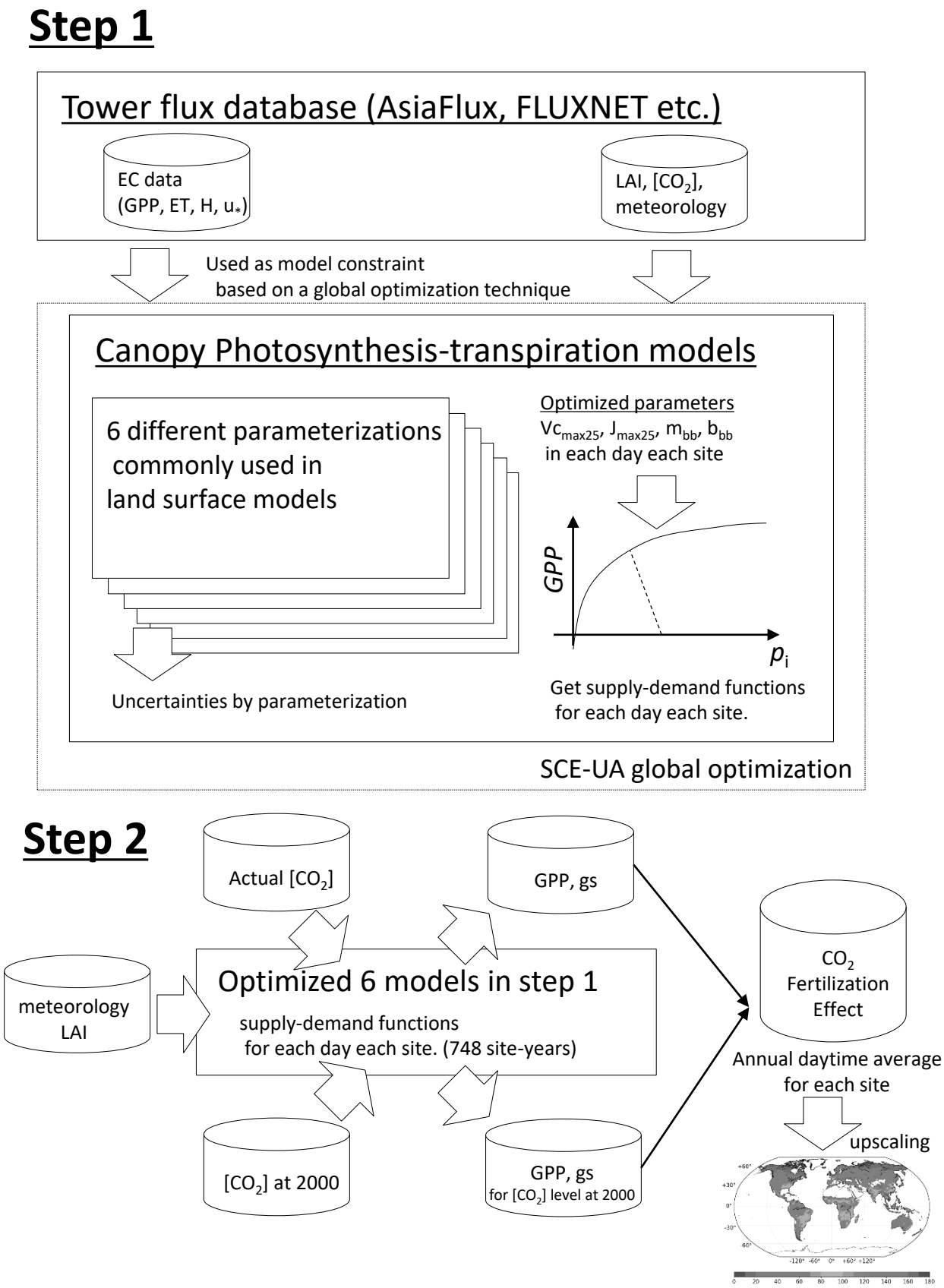


Schematic diagram for estimating the $CO_2$ fertilization effect. The scheme consists of two steps: 1) estimating supply-demand functions for each day for each site optimizing the canopy photosynthesis-transpiration model using eddy covariance data, and 2) estimating $CO_2$ fertilization effect using the optimized model as sensitivity for different $CO_2$ concentration levels. Step 2 includes upscaling of the $CO_2$ fertilization effects using global climate and satellite data with the random forest regression.

# Figure S3

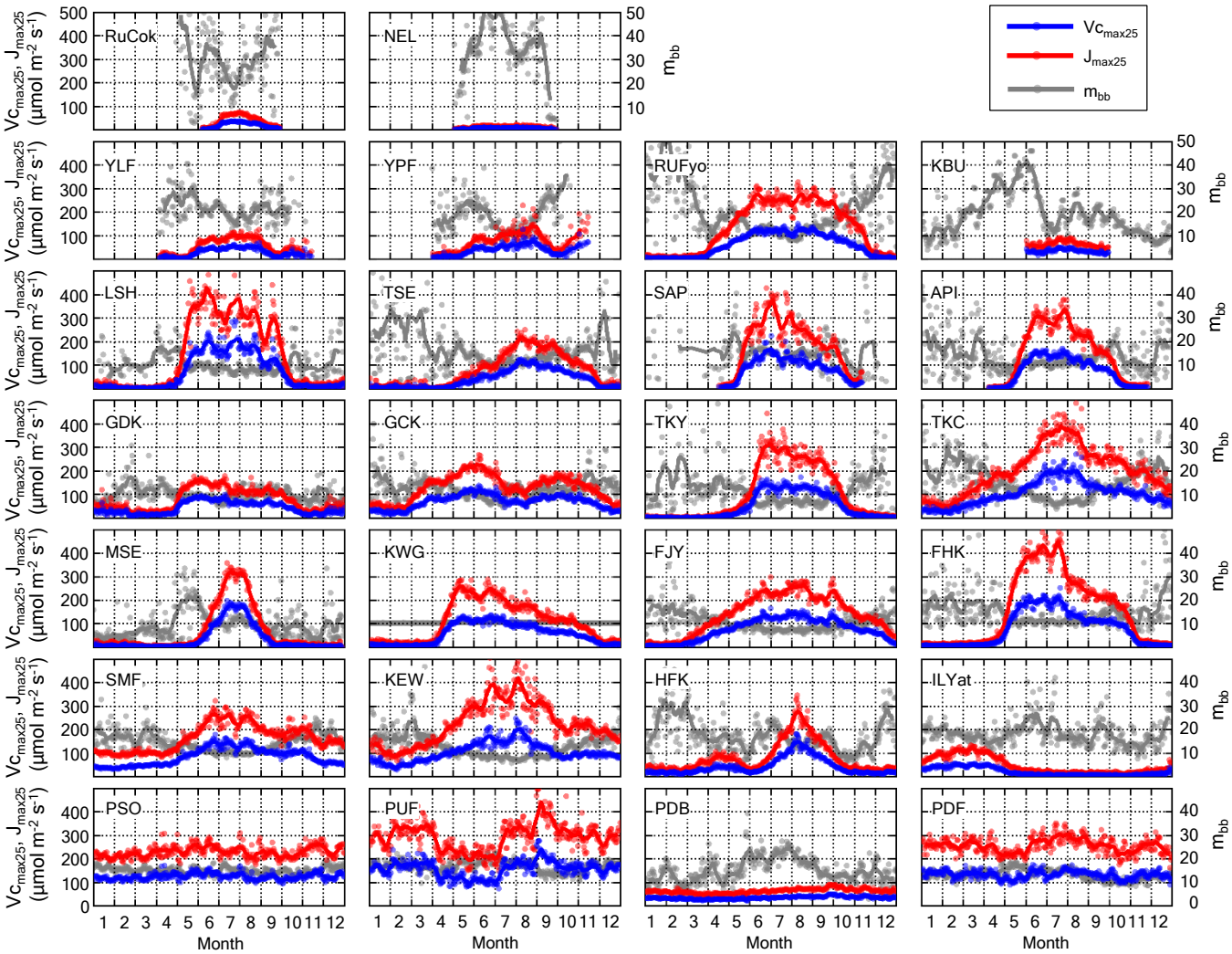


Mean seasonal variations in the optimized parameters of big-leaf $Vc_{max25}$, $J_{max25}$, and $m_{bb}$ for study sites where eddy covariance data covered more than five years. Dots represent the mean seasonal variation, and lines represent its 14-days moving mean. The $m_{bb}$ in KWG was assumed as the growing-season mean for SAP due to lack of ET measurements.

# Figure S3

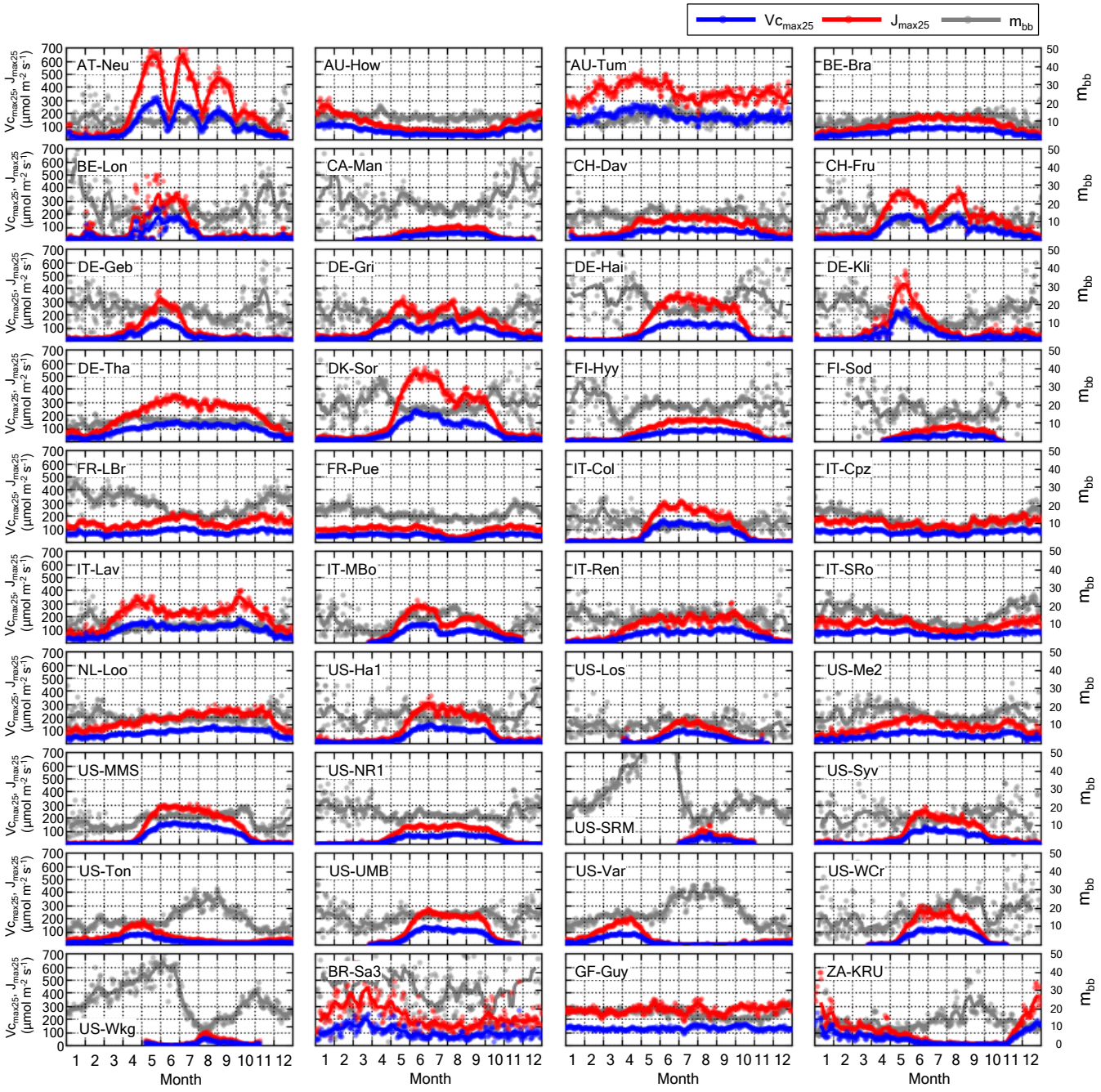


Continued.

# Figure S4

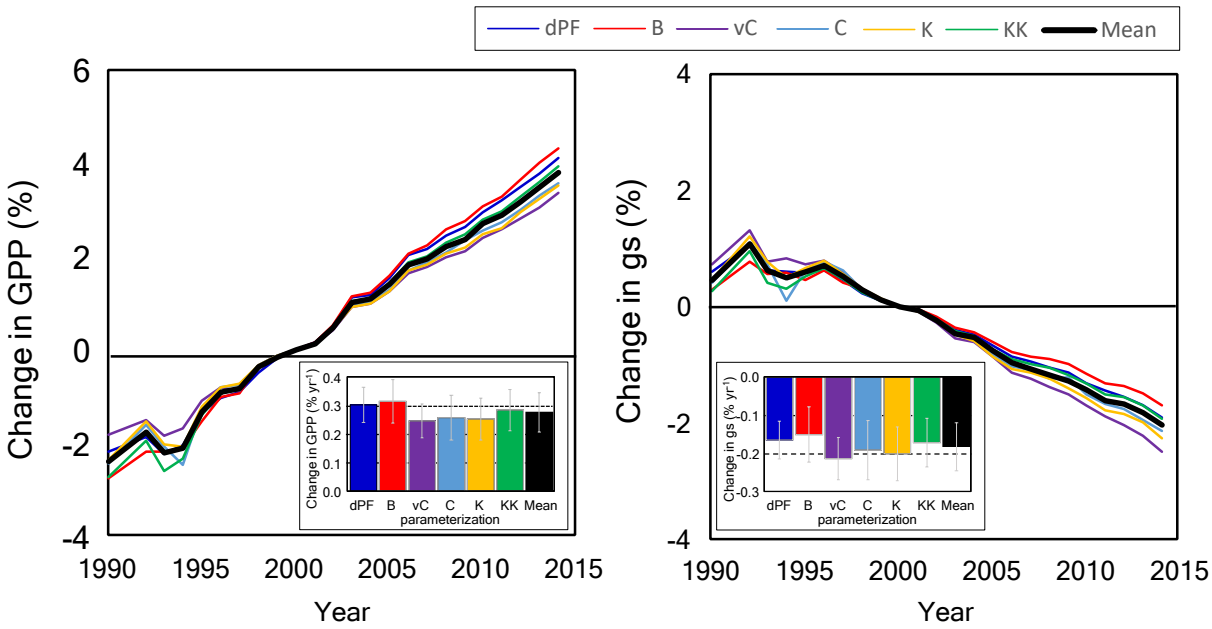


Fractional changes in gross primary productivity (GPP), and canopy-integrated stomatal conductance (gs), associated with rising $CO_2$ concentration. The $CO_2$ fertilization effect was quantified, with $CO_2$ concentration in 2000 as a baseline. Analysis was done based on the coupled photosynthesis and stomatal conductance model with six different parameterizations: dPF (de Pury and Farquhar, 1997), B (Bernacchi et al., 2001, 2003), C (Collatz et al., 1991), vC (von Caemmerer et al., 2009), K (Kosugi et al., 2003), KK (Kattge and Knorr, 2007). The individual lines represent the ensemble mean of the $CO_2$ fertilization effect of different sites in a respective year. The inset shows the mean rates of change in GPP and gs of the individual sites.

# Figure S5

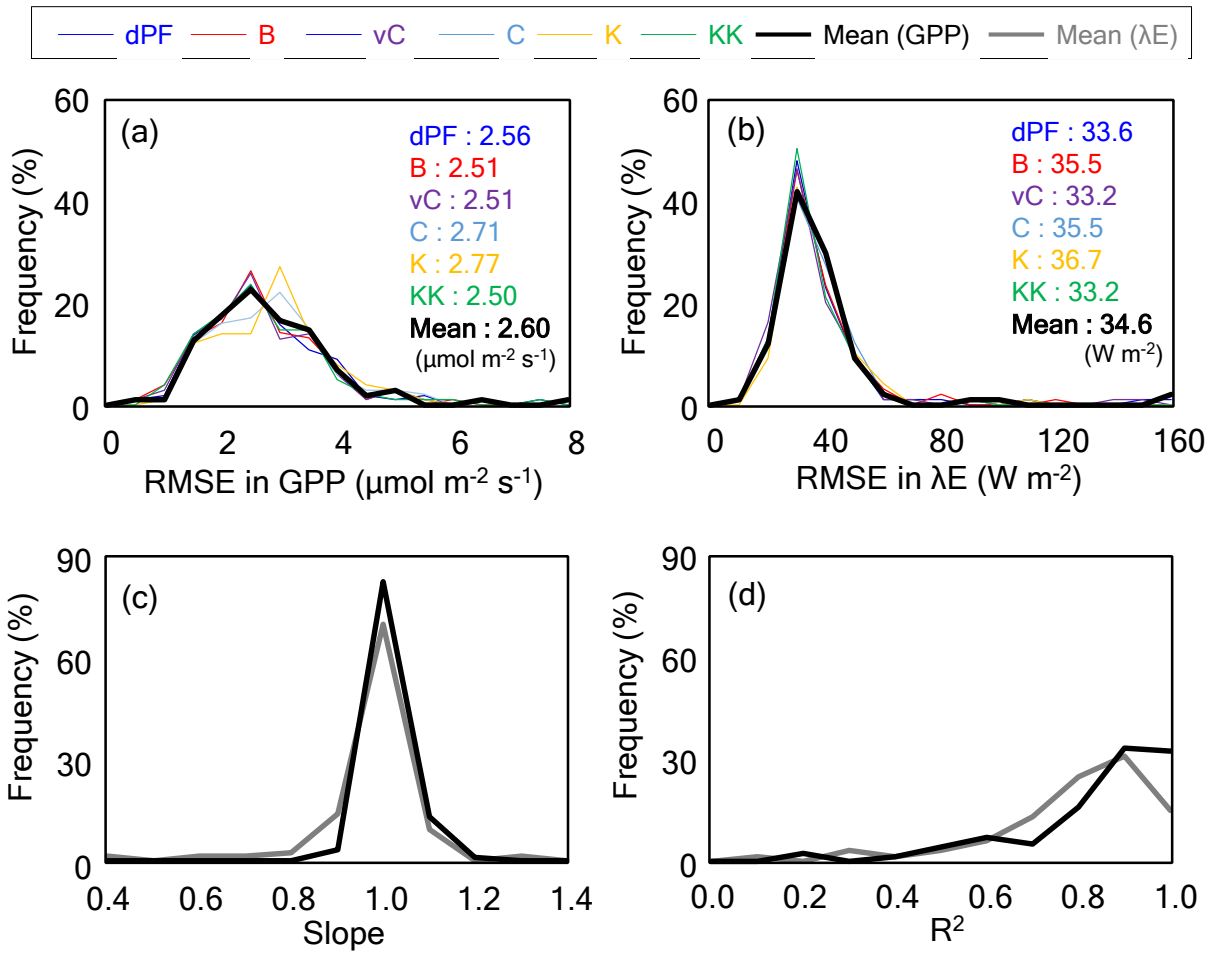


Frequency distributions of statistics for the optimized model among study sites: root mean square error (RMSE) of gross primary productivity (GPP) (a), RMSE of latent heat flux (λE) (b), slope (observation = slope * model + 0.0) (c), and determination coefficient ($R^2$) (d). Statistics for each site were estimated based on the comparison of daytime mean fluxes, i.e. when photosynthetically active photon flux density was greater than 500 μmol $m^{-2}$ $s^{-1}$. The colors in (a) and (b) represent estimates using different biochemical parameterizations: dPF (de Pury and Farquhar, 1997), B (Bernacchi et al., 2001, 2003), C (Collatz et al., 1991), vC (von Caemmerer et al., 2009), K (Kosugi et al., 2003), KK (Kattge and Knorr, 2007), and mean across the six models. Numbers in (a) and (b) were mean RMSE by different biochemical parameterizations. The statistics show that performance of the different parameterizations is similar, but RMSE is 3.3% smaller in B, and 5.4% higher in K than mean of the six parameterizations.

# Figure S6

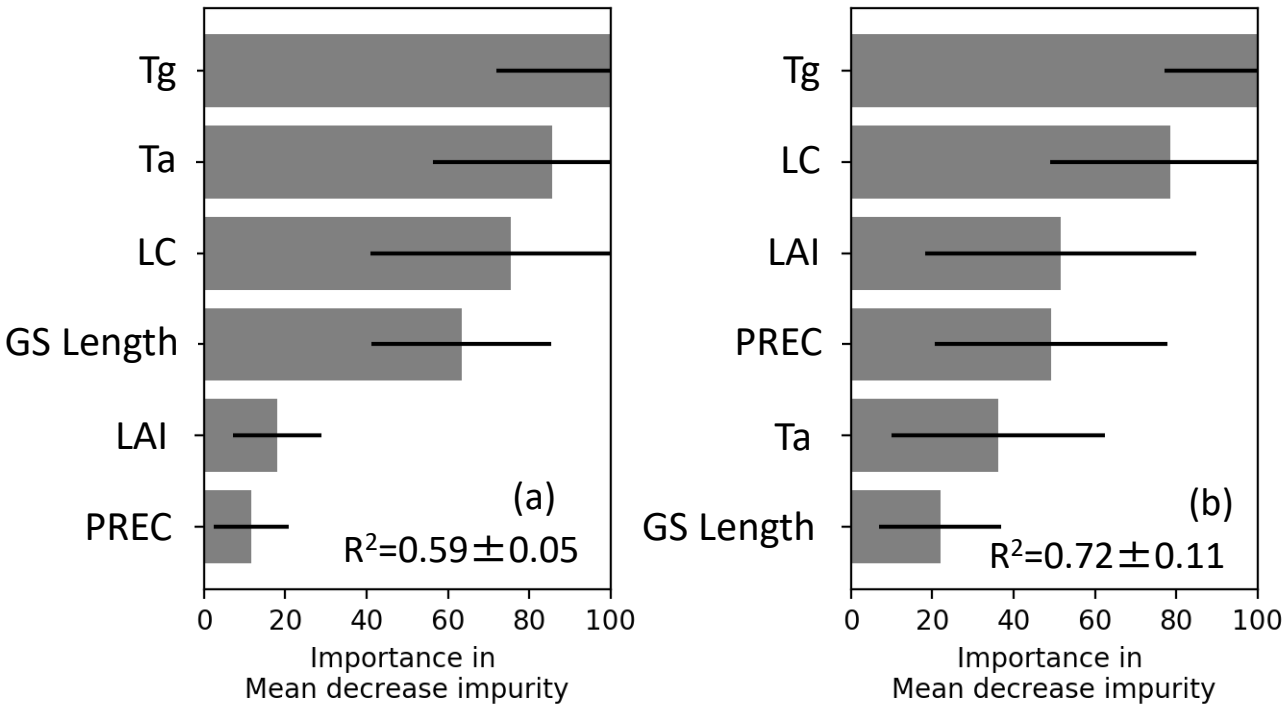


Relative importance of environmental variables to spatial variations in the $CO_2$ fertilization effect per change in [$CO_2$] for gross primary productivity (GPP) (a) and canopy-integrated stomatal conductance (gs) (b) based on mean decrease impurity by the random forest: annual air temperature (Ta), growing season temperature (Tg), land cover (LC; forest or non-forest), length of growing season when air temperature is greater than 5$^{o}$C (GS Length), LAI, and annual sum of precipitation (PREC). Error bars represent the standard deviation of the output of 20 models with different hyper parameters.

# Figure S7

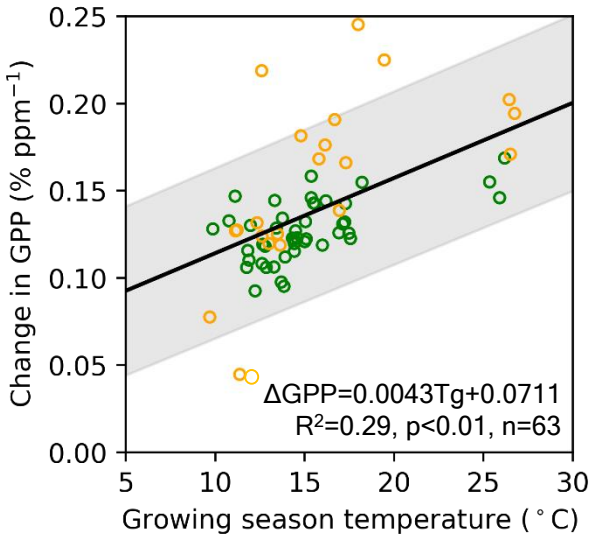


Relationship between mean growing season air temperature ($Ta_{grow}$) and fractional change in GPP associated with rising atmospheric $CO_2$ concentration (ΔGPP). The relationship was examined using sites data with an availability of at least four years. $Ta_{grow}$ is defined as the annual mean temperature when daily temperature is higher than 5°C. Green and yellow represent changes for forests and non-forest sites, respectively.

# Figure S8

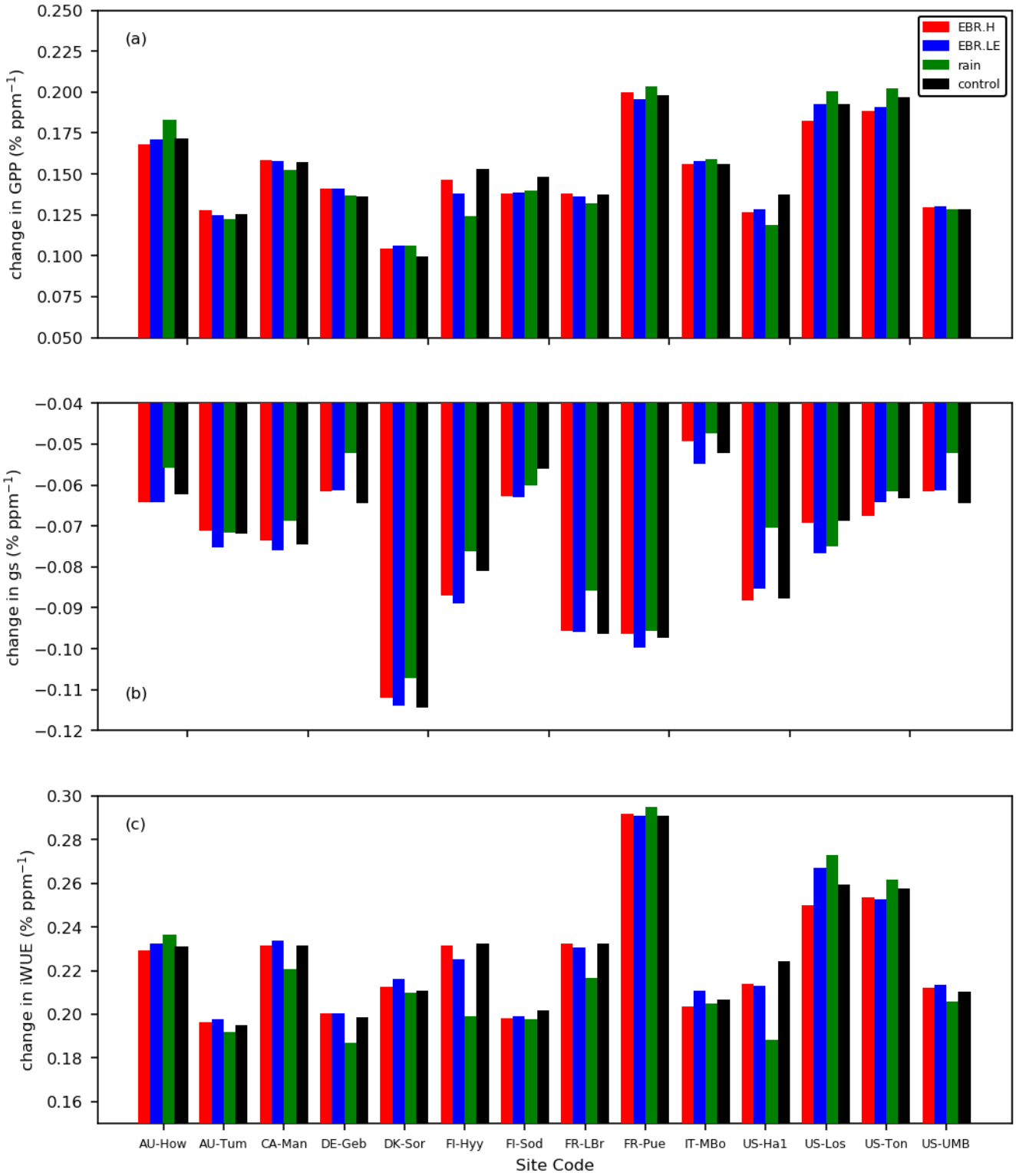


The $CO_2$ fertilization effect of gross primary productivity (GPP) (a), canopy-integrated stomatal conductance (gs) (b), and intrinsic water use efficiency (iWUE) (c) by different assumptions: energy imbalance was caused by sensible heat flux, energy imbalance was caused by latent heat flux, data has to be rejected after 24 hours after rain event for canceling intercepted evaporation, and control simulation. The $CO_2$ fertilization effects was estimated optimizing a submodel (de Pury and Farquhar, 1997).

*Environmental Research Letters*

# Supporting Information for

## Inferring $CO_2$ fertilization effect based on global monitoring land-atmosphere exchange with a theoretical model

Masahito Ueyama*, Graduate School of Life and Environmental Sciences, Osaka Prefecture University, 1-1, Gakuen-cho, Nakaku, Sakai, 599-8531 Japan

Kazuhito Ichii[1,2], (1) Center for Environmental Remote Sensing, Chiba University, 1-33 Yayoi-cho, Inage-ku, Chiba, 263-8522 Japan; (2) Center for Global Environmental Change, National Institute for Environmental Studies, 16-2 Onokawa, Tsukuba, 305-8506 Japan

Hideki Kobayashi, Institute of Arctic Climate and Environment Change Research, Japan Agency for Marine-Earth Science and Technology, 3173-25 Showa-machi, Kanazawa-ku, Yokohama, 236-0001 Japan

Tomo'omi Kumagai[1, 2], (1) Graduate School of Agricultural and Life Sciences, The University of Tokyo, 1-1-1 Yayoi, Bunkyo-ku, Tokyo, 113-8657 Japan; (2) Institute for Space-Earth Environmental Research, Nagoya University, Furo-cho, Chikusa-ku, Nagoya, 464-8601 Japan

Jason Beringer, School of Agriculture and Environment, The University of Western Australia, 35 Stirling Hwy, Crawley, Perth WA, 6009 Australia

Lutz Merbold, Mazingira Centre, International Livestock Research Institute (ILRI), PO Box 30709, 00100 Nairobi, 30709 Kenya

Eugénie S. Euskirchen, Institute of Arctic Biology, University of Alaska Fairbanks, 311 Irving 1 Building, Fairbanks, 757000 USA

Takashi Hirano, Research Faculty of Agriculture, Hokkaido University, Kita 8, Nishi 5, Kita-ku, Sapporo, 060-0808 Japan

Luca Belelli Marchesini, Department of Sustainable Agro-ecosystems and Bioresources, Research and Innovation Centre, Fondazione Edmund Mach, San Michele all'Adige, Italy

Dennis Baldocchi, Department of Environmental Science, Policy and Management, University of California, Berkeley, 345 Hilgard Hall, Office, Berkeley, CA 94720-3110 USA

Taku M. Saitoh, River Basin Research Center, Gifu University, 1-1 Yanagido, Gifu, Japan 501-1193

Yasuko Mizoguchi, Hokkaido Research Center, Forestry and Forest Products Research Institute, 7 Hitsujigaoka, Toyohira-ku, Sapporo, 062-8516 Japan

Keisuke Ono, Institute for Agro-Environmental Sciences, National Agriculture and Food Research organization, 3-1-3 Kannondai, Tsukuba, 305-8604 Japan

Joon Kim, Department of Landscape Architecture & Rural Systems Engineering, Interdisciplinary Program in Agricultural & Forest Meteorology, Seoul National University, 1 Gwanak-ro, Gwanak-gu, Seoul, 08826 Korea

Andrej Varlagin, A.N. Severtsov Institute of Ecology and Evolution RAS, Leninsky pr.33, Moscow, 119071 Russia

Minseok Kang, National Center for AgroMeteorology, 1, Gwanak-ro, Gwanak-gu, Seoul 08826, Korea

Takanori Shimizu, Forestry and Forest Products Research Institute, 1 Matsunosato, Tsukuba, 305-8687 Japan, Japan

Yoshiko Kosugi, Graduate School of Agriculture, Kyoto University, Yoshidahonmachi, Sakyo-ku, Kyoto, 606-8501 Japan

Marion Syndonia Bret-Harte, Institute of Arctic Biology, University of Alaska Fairbanks, 311 Irving 1 Building, Fairbanks, 757000 USA

Takashi Machimura, Graduate School of Engineering, Osaka University, 1-1 Yamadaoka, Suita, 565-0871 Japan

Yojiro Matsuura, Center for International Partnerships and Research on Climate Change, Forestry and Forest Products Research Institute, 1 Matsunosato, Tsukuba, Japan 305-8687, Japan

Takeshi Ohta, Professor emeritus, Nagoya University, Furo-cho, Chikua-ku, Nagoya, 464-8601 Japan

Kentaro Takagi, Field Science Center for Northern Biosphere, Hokkaido University, 135 Toikanbetsu, Horonobe-cho, Teshio-gun, 098-2943 Japan

Satoru Takanashi, Kansai Research Center, Forestry and Forest Products Research Institute, 68 Nagaikyutarou, Momoyama-cho, 612-0855 Japan

Yukio Yasuda, Forestry and Forest Products Research Institute, 1 Matsunosato, Tsukuba, 305-8687 Japan

Corresponding author: Masahito UEYAMA (ueyama@envi.osakafu-u.ac.jp)

**Uncertainty analysis associated with energy imbalance and evaporation contributions**

We quantified the range of uncertainties associated with the energy imbalance of observed data, and intercepted evaporation from the wet surface. Uncertainties by the energy imbalance and intercepted evaporation were estimated using data from selected 14 sites from FLUXNET2015. We quantified a range of the uncertainties for energy imbalance by testing two extreme assumptions (Knauer et al., 2018): 1) all errors were in sensible heat flux and 2) all errors were in latent heat flux. We also quantified uncertainties due to intercepted evaporation, by rejecting data under wet conditions which was defined by 1-day after a rain event (Knauer et al., 2018). The $CO_2$ fertilization was quantified by optimizing the model with corrected heat fluxes or strict criterion for wet conditions as input. Systematic error was estimated based on a Student's t-test compared with our baseline results. Random errors were estimated as the coefficient of variance in the $CO_2$ fertilization effects among the 14 sites. Uncertainties in $CO_2$ fertilization effect due to energy imbalance and wet surface conditions was small (Fig. S8). The magnitude of the error was less than one tenth the size the magnitude of the $CO_2$ fertilization effects. Energy imbalance induced no systematic error for quantifying the $CO_2$ fertilization effects, with a coefficient of variance: 5.5 % for GPP, 8.1 % for gs, and 3.0 % for iWUE. The $CO_2$ fertilization effects in gs and iWUE systematically decreased 7.9 ± 10.0% and 4.3 ± 6.4%, respectively ($p < 0.05$), with the criterion for wet surface conditions compared against the baseline. Thus, the systematic errors in gs and iWUE were considered as extending one tail of error bars by the systematic errors in Fig. 1 and 3.

**Model**

*A1. Model*

We developed a sun/shade model (inverse Big-Leaf Model for Eddy Covariance; iBLM-EC version 2.0) with coupled photosynthesis (Farquhar et al., 1980) and stomatal conductance (Ball et al., 1987) sub-models for inverting ecosystem-scale ecophysiological parameters: a maximum carboxylation rate at 25 ºC ($Vc_{max25}$), a maximum electron transport rate at 25 ºC ($J_{max25}$), and stomatal conductance parameters ($m_{bb}$ and $b_{bb}$ in Ball et al., 1987). Input variables are wind speed, incoming and reflected photosynthetically active photon flux density (PPFD), air temperature, relative humidity, rainfall, atmospheric pressure, atmospheric carbon dioxide concentration [$CO_2$], net radiation, ground heat flux, friction velocity ($u_*$), sensible and latent heat fluxes, gross primary productivity (GPP), and leaf area index (LAI). Reflected PPFD is calculated based on the radiation transfer model (Ryu et al., 2011).

*A1-1. Photosynthesis model*

Based on the biochemical model (Farquhar et al., 1980), the photosynthetic rate ($A$) is

determined as the minimum rate of Rubisco-limited photosynthesis ($A_v$) and RuBP-limited photosynthesis ($A_j$):

$$A = \min\{A_v, A_j\} - R_l \tag{A1}$$

$$A_v = Vc_{max} \frac{p_i - \Gamma_*}{p_i + K_c(1 + p_o / K_o)} \tag{A2}$$

$$A_j = J \frac{p_i - \Gamma_*}{4p_i + 8\Gamma_*} \tag{A3}$$

where $R_l$ is mitochondrial respiration in light, $Vc_{max}$ is the maximum carboxylation rate, $J$ is the electron transport rate, $\Gamma_*$ is the $CO_2$ compensation point for photosynthesis in the absence of mitochondrial respiration, $p_i$ is intercellular $CO_2$ partial pressure, $p_o$ is intercellular $O_2$ partial pressure, and $K_c$ and $K_o$ are Michaelis-Menten constants. The variables $Vc_{max}$, $J$, $K_c$, $K_o$, $\Gamma_*$, and $R_l$ change with leaf temperature, and are often parameterized with various types of kinetic functions. We performed simulations with the biochemical model using six different parameterizations (Table A1 in Ueyama et al., 2016) from de Pury & Farquhar (1997), Bernacchi et al. (2001, 2003), Collatz et al. (1991), von Caemmerer et al. (2009), Kosugi et al. (2003), and Kattge & Knorr (2007). While kinetic functions, such as the Arrhenius-type equation, were similar across the six models with only slightly different parameterizations, a model by Kattge & Knorr (2007) considered the acclimation of $Vc_{max}$ to growth temperature in the kinetic functions. To introduce a realistic gradual transition from one limitation to another in Eq. A1, we applied an empirical quadratic function proposed by Collatz et al. (1991).

We used a set of kinetic functions and related parameters for the photosynthesis model, for quantifying uncertainties by parameters that were not constrained by data. The parameters included the maximum carboxylation rate ($Vc_{max}$), the maximum electron transport rate ($J_{max}$), Michaelis-Menten constants ($K_c$, and $K_o$), the $CO_2$ compensation point for photosynthesis in the absence of mitochondrial respiration ($\Gamma_*$), and mitochondrial respiration in light ($R_l$) change with leaf temperature (Table A1 in Ueyama et al., 2016). Basic equations for each model were originally proposed by de Pury & Farquhar (1997), Bernacchi et al. (2001, 2003), Collatz et al. (1991), von Caemmerer et al. (2009), Kosugi et al. (2003), and Kattge & Knorr (2007), but we slightly modified the models and parameterization (Table A1 in Ueyama et al., 2016) from the original ones upon introducing our inversion scheme (shown in section A2).

*Model 1 based on de Pury and Farquhar (1997)*

Temperature dependence of $Vc_{max}$ (μmol mol$^{-1}$), $K_c$ (Pa), $K_o$ (Pa), and $R_l$ (μmol mol$^{-1}$) are modeled by the Arrhenius function.

$$k_T = k_{25} \exp\left[ E_a \frac{T_K - 298}{298 \cdot R \cdot T_K} \right] \tag{A4}$$

where $k_T$ and $k_{25}$ are variables (e.g., $Vc_{max}$, $K_c$, $K_o$, or $R_l$) at a given temperature and the reference temperature of 25 °C, respectively. $T_K$ is leaf temperature in Kelvin, and $E_a$ is the activation energy (J mol$^{-1}$) (Table A1 in Ueyama et al., 2016), and R is the universal gas constant (8.314 J mol$^{-1}$ K$^{-1}$). The temperature dependence of $\Gamma_*$ (Pa) and $J_{max}$ (μmol mol$^{-1}$) are described as follows:

$$\Gamma_* = 3.69 + 0.188(T_K - 298) + 0.0036(T_K - 298)^2, \tag{A5}$$

$$J_{max} = J_{max25} \exp\left[ \frac{(T_K - 298)E_a}{RT_K \cdot 298} \right] \left[ \frac{1 + \exp\left( \frac{S \cdot 298 - E_d}{R \cdot 298} \right)}{1 + \exp\left( \frac{S \cdot T_K - E_d}{R \cdot T_K} \right)} \right]. \tag{A6}$$

where $J_{max25}$ is the maximum electron transport rate at 25 °C (μmol mol$^{-1}$), S is an entropy term (J K$^{-1}$ mol$^{-1}$), and $E_d$ is the deactivation energy (J mol$^{-1}$) (Table A1 in Ueyama et al., 2016). The electron transport rate is described as follows:

$$\theta_I J^2 - (I_{le} + J_{max})J + I_{le} J_{max} = 0 \tag{A7}$$

$$I_{le} = 0.5 \cdot I_l (1 - f) \tag{A8}$$

where $\theta_I$ is the curvature of leaf response of electron transport to irradiance (0.7), $J$ is the electron transport rate, $I_{le}$ is PPFD effectively absorbed by PSII, $I_l$ is incoming PPFD, and $f$ is the spectral correction factor (0.15).

*Model 2 based on Bernacchi et al. (2001, 2003)*

Temperature dependence of $Vc_{max}$ (μmol mol$^{-1}$), $J_{max}$ (μmol mol$^{-1}$), $K_c$ (μmol mol$^{-1}$), $K_o$ (μmol mol$^{-1}$), $\Gamma_*$ (μmol mol$^{-1}$), and $R_l$ (μmol mol$^{-1}$) are modeled by the following function (Bernacchi et al., 2001, 2003) (Table A1 in Ueyama et al., 2016).

$$k_T = \exp\left(c - \frac{E_a/1000}{RT_K}\right) \tag{A9}$$

where c is a scaling constant (Table A1 in Ueyama et al., 2016). The electron transport rate is described as follows:

$$J = \frac{I_{le} + J_{max} - \sqrt{(I_{le} + J_{max})^2 - 4\Theta_{PSII} I_{le} J_{max}}}{2 \cdot \Theta_{PSII}} \tag{A10}$$

$$\Theta_{PSII} = 0.76 + 0.018T - 3.7e^{-4}T^2 \tag{A11}$$

$$I_{le} = 0.5 \cdot I_l \cdot a_l \cdot \Phi_{PSIImax} \tag{A12}$$

$$\Phi_{PSIImax} = 0.353 + 0.022T - 3.4e^{-2}T^2 \tag{A13}$$

where $T$ is leaf temperature in degree Celsius, $\Theta_{PSII}$ is the convexity term for electron transport rates (dimensionless), $a_l$ is the total leaf absorbance (dimensionless), and $\Phi_{PSIImax}$ is the apparent quantum yield of $CO_2$ assimilation (dimensionless).

*Model 3 based on van Caemmerer et al. (2009)*

Temperature dependence of $Vc_{max}$ (μmol mol$^{-1}$), $K_c$ (Pa), $K_o$ (Pa) , $\Gamma_*$ (Pa), and $R_l$ (μmol mol$^{-1}$) are modeled by the Arrhenius function (Eq. A4) with different parameterization (Table A1 in Ueyama et al., 2016). The electron transport is based on Eq. A6 and A7, where $I_{le}$ is defined as:

$$I_{le} = 0.5 \cdot 0.85 \cdot I_l (1 - f) \tag{A14}$$

*Model 4 based on Collatz et al. (2001)*

Temperature dependence of $Vc_{max}$ (μmol mol$^{-1}$), $J_{max}$ (μmol mol$^{-1}$), $K_c$ (Pa), $K_o$ (Pa), $CO_2/O_2$ specificity ratio ($\tau$) (dimensionless), and $R_l$ (μmol mol$^{-1}$) are modeled by the $Q_{10}$ function.

$$k_T = k_{25} Q_{10}^{(T-25)/10} \tag{A15}$$

where $Q_{10}$ is the relative change in the parameter for a 10 °C change in temperature. In this model, the reduction of $Vc_{max}$ under high temperatures is introduced in the following formula:

$$Vc_{max} = Vc_{max0} \left\{ 1 + \exp\left[ \frac{-220 + 703(T + 273)}{R(T + 273)} \right] \right\}^{-1} \tag{A16}$$

where $Vc_{max0}$ is $Vc_{max}$ calculated using Eq. A15. Temperature inhibition at high temperature is also introduced for $R_l$.

$$R_l = R_{l0} \{1 + \exp[1.3(T - 55)]\}^{-1} \tag{A17}$$

where $R_{l0}$ is $R_l$ calculated using Eq. A15. For calculating the electron transport rate, we used the model (Eq. A6 to A8) by de Pury & Farquhar (1997).

*Model 5 based on Kosugi et al. (2003)*

Temperature dependence of $Vc_{max}$ (μmol mol$^{-1}$) and $J_{max}$ (μmol mol$^{-1}$) is calculated as follows:

$$Vc_{max} = Vc_{max25} \frac{\exp\left[ \left( 1 - \frac{298}{T_K} \right) \frac{E_a}{R \cdot 298} \right]}{1 + \exp\left[ \frac{S \cdot T_K - E_d}{R \cdot T_K} \right]} \tag{A18}$$

The temperature dependence of $K_c$ (Pa), $K_o$ (Pa), $\tau$, and $R_l$ (μmol mol$^{-1}$) are modeled by the Arrhenius function.

$$k_T = k_{25} \exp\left[\left(1 - \frac{298}{T_K}\right)\frac{E_a}{R \cdot 298}\right] \quad \text{(A19)}$$

For calculating the electron transport rate, we used the model (Eq. A6 to A8) by de Pury & Farquhar (1997).

*Model 6 based on Kattge and Knorr (2007)*

Temperature dependence of $Vc_{max}$ (μmol mol$^{-1}$) and $J_{max}$ (μmol mol$^{-1}$) are calculated using Eq. A6, where $Vc_{max}$ is also calculated using same temperature dependence function with different parameters. Temperature dependence of $R_l$ (μmol mol$^{-1}$) is calculated by Eq. A9 with a different parameterization (Table A1 in Ueyama et al., 2016). Temperature dependence of $K_c$ (μmol mol$^{-1}$), $K_o$ (μmol mol$^{-1}$), and $\Gamma_*$ (μmol mol$^{-1}$) are modeled by Eq. A4. The electron transport rate is described as follows:

$$J = \frac{I_{le} + J_{max} - \sqrt{(I_{le} + J_{max})^2 - 4 \cdot 0.9 \cdot I_{le} J_{max}}}{2 \cdot 0.9} \quad \text{(A20)}$$

$$I_{le} = 0.3 \cdot I_l \quad \text{(A21)}$$

*A1-2. Stomatal conductance model*

Based on Ball et al. (1987), stomatal conductance are modelled:

$$g_{sw} = m_{bb} \frac{A}{c_s} rh_s + b_{bb} \quad \text{(A22)}$$

where $g_{sw}$ is stomatal conductance to water vapor, $rh_s$ is relative humidity at the leaf surface (Eq. A32), $c_s$ is $CO_2$ concentration at the leaf surface, $m_{bb}$ is an empirical parameter for a dimensionless slope, and $b_{bb}$ is an empirical parameter for the zero intercept when net photosynthetic rate is equal or less than zero. Once $g_{sw}$ was obtained, water vapor flux was calculated using the product of total conductance, and vapor pressure deficit (VPD) at the leaf surface. To solve equations A1 – 3, and A22 for photosynthesis and stomatal conductance simultaneously, we used an iteration rather than a cubic equation that was used in the previous version of our model (Ueyama et al., 2016).

*A1-3. Sun/Shade radiation transfer model*

Canopy radiation transfer was based on a sun/shade model (de Pury & Farquhar, 1997; Ryu et al., 2011). The direct and diffuse portions of radiation were partitioned based on the method of Weiss & Norman (1985), for solving sun/shade radiation transfer model. Photosynthesis and transpiration were separately calculated for sun and shade leaves. An ecosystem-scale parameter of $X_{eco}$ (specifically, $Vc_{max25}$, $J_{max25}$, and $b_{bb}$) can be divided into ecosystem-scale parameters of $X_{sun}$ for sun leaf and $X_{shade}$ for shade leaf.

$$\begin{aligned} X_{eco} &= X_{sun} + X_{shade} \\ &= x_0 L_{sun} + x_0 L_{shade} \end{aligned} \quad \text{(A23)}$$

where $x_0$ are the parameter for unit leaf area, $L_{sun}$ is sunlit leaf area index, and $L_{shade}$ is shaded leaf area index. Assuming the proximity of vertical distribution among leaf nitrogen and irradiance, $x_0$ is written as:

$$X_{sun} = X_{eco} \frac{\dfrac{\Omega}{k_n + k_b \Omega L}\left[1 - \exp\left(-\left(k_n + k_b \Omega L\right)\right)\right]}{\dfrac{1}{k_n}\left[1 - \exp\left(-k_n\right)\right]} \quad \text{(A24)},$$

$$L_{sun} = \frac{\left[1 - \exp\left(-k_b \Omega L\right)\right]}{k_b} \quad \text{(A25)},$$

$$x_0 = X_{sun} / L_{sun} \quad \text{(A26)}$$

where $L$ is leaf area index ($m^2$ $m^{-2}$), $k_b$ is the extinction coefficient for beam PPFD, $k_n$ is the nitrogen extinction coefficient (de Pury & Farquhar, 1997; Lloyd et al., 2010), and $\Omega$ is the clumping index (Table A1; He et al., 2012). The extinction coefficient, $k_b$, is calculated as

$$k_b = G(\theta) / \cos\theta \quad \text{(A27)}$$

where $G$ is the G-function defined as the projection coefficient of foliage area on the plane

perpendicular to the view direction (Ross, 1981), and $\theta$ is the solar zenith angle. We used a look-up-table among $G$ and $\theta$ by assuming leaf angle distribution as spherical, planophile, or erectrophile (Pisek et al., 2013).

The nitrogen extinction coefficient, $k_n$, was estimated based on a relationship to maximum carboxylation rate per unit leaf area at a top of canopy, $vc_{max25}$ (Lloyd et al., 2010).

$$\log_e(k_n) = 0.00963\, vc_{max25} - 2.43 \tag{A28}$$

By solving $k_n$ and $vc_{max25}$ simultaneously, $vc_{max25}$ was determined from big-leaf $Vc_{max25}$ by iteratively solving Eq. A24 to A28.

*A1-4. Surface conditions at big leaf*

Surface meteorological conditions near the big-leaf canopy were estimated from micrometeorological observations. Aerodynamic conductance of sensible heat ($g_b$; m s$^{-1}$) was estimated as

$$g_b = 1/\left(u/u_*^2 + B^{-1}/u_*\right) \tag{A29}$$

where $u$ is horizontal wind velocity (m s$^{-1}$), $u_*$ is friction velocity (m s$^{-1}$), and $B^{-1}$ is the parameter related to the roughness height (dimensionless). According to Lhomme et al. (2000), $B^{-1}$ can be estimated using LAI ($L$; m$^2$ m$^{-2}$) as

$$B^{-1} = a_6 L^6 + a_5 L^5 + a_4 L^4 + a_3 L^3 + a_2 L^2 + a_1 L^1 + a_0 \tag{A30}$$

where $a_0$ (8.9667), $a_1$ (16.127), $a_2$ (-36.403), $a_3$ (27.343), $a_4$ (-9.9967), $a_5$ (1.8013), $a_6$ (-0.128) are empirical constants. Once $g_b$ was estimated, leaf temperature ($T_{leaf}$; K) was inversely estimated using sensible heat flux ($H$; W m$^{-2}$), and air temperature ($T_{air}$; K) as

$$H = c_p \rho_{air} g_b \left(T_{leaf} - T_{air}\right) \tag{A31}$$

where $c_p$ is the specific heat (1004 J K$^{-1}$ kg$^{-1}$), and $\rho_{air}$ is air density (kg m$^{-3}$).

Relative humidity at the leaf surface is calculated based on Su et al. (1996).

$$rh_s = \frac{g_b Q_{air} + g_c Q_{leaf}}{g_b Q_{leaf} + g_c Q_{leaf}} \quad \text{(A32)}$$

where $Q_{air}$ is mixing ratio (kg kg$^{-1}$), $Q_{leaf}$ is mixing ratio at leaf (kg kg$^{-1}$), and $g_c$ is canopy conductance (m s$^{-1}$). $Q_{leaf}$ is calculated from saturation vapor pressure at given leaf temperature. $g_c$ is calculated based on the Penman-Monteith equation (Monteith, 1965).

$$g_c^{-1} = \left(\frac{\Delta}{\gamma}\frac{H}{\lambda E} - 1\right) g_b^{-1} + \frac{\rho_{air} c_p D}{\gamma \lambda E} \quad \text{(A33)}$$

where Δ is the rate of change of saturation vapor pressure with temperature (hPa K$^{-1}$), γ is the psychrometric constant (hPa K$^{-1}$), $D$ is the vapor pressure deficits (hPa), and λE is latent heat flux (W m$^{-2}$).

*A1-6. Partitioning evapotranspiration*

Measured evapotranspiration, *ET*, from the eddy covariance method was partitioned into transpiration, *T*. First, we only use dry canopy; wet conditions during rain and within one hour after rain were not used in this study. Then, dry canopy evapotranspiration was partitioned using following equations. For grassland, tundra, and all croplands except rice paddy, a known ratio between evapotranspiration and transpiration (Wang et al., 2014) was used.

$$\frac{T}{ET} = c_1 e^{L + c_2} \quad \text{(A34)}$$

where $c_1$ and $c_2$ are empirical constant. Values of $c_1$ and $c_2$ for grassland and tundra are 0.77 and 0.10, respectively; those for cropland are 0.91 and 0.07, respectively. For rice paddy (Sakuratani & Horie, 1985), transpiration was partitioned as:

$$\frac{T}{ET} = \left(1.0 - e^{-0.4L}\right) \quad \text{(A35)}$$

For forest ecosystems, soil evaporation was estimated based on potential evaporation at the soil surface. The radiation transfer of PPFD and infrared radiation was separately calculated for

estimating net radiation at the soil surface (Ryu et al., 2011), with transpiration then estimated by subtracting soil evaporation.

*A2. Optimization*

The model parameters were determined using a globally optimization method: the shuffled complex evolution method developed at the University of Arizona (SCE-UA; Duan et al., 1992, 1993, 1994). For successful global optimization, the SCE-UA introduces four concepts: a combination of random and deterministic approaches, clustering, systematic evolution, and competitive evolution. The SCE-UA was developed and used successfully to determine parameters of hydrological models. In this study, we used the method with the settings recommended in Duan et al. (1992, 1994).

The model parameters of $Vc_{max25}$, ratio of $J_{max25}$ to $Vc_{max25}$ ($J_{max25}/Vc_{max25}$), $m_{bb}$ and $b_{bb}$ were determined using half-hourly GPP and λE. Parameters were determined each day using an eight-day moving window for given parameter ranges with 0.1 ~ 700 μmol m$^{-2}$ s$^{-1}$ for $Vc_{max25}$, 1.8 ~ 2.7 for $J_{max25}/Vc_{max25}$ (von Caemmerer et al., 2009; Wang et al., 2007; Wullschleger, 1993), 0.1 ~ 100 for $m_{bb}$ and 0 ~ 1 mmol m$^{-2}$ s$^{-1}$ for $b_{bb}$. Applying seasonally varying parameters with a moving window allows consideration of changes in physiological traits, such as periodic drought stress. First, $m_{bb}$ and $b_{bb}$ were determined by minimizing the root mean square error (RMSE) between observed and modeled transpiration, where observed GPP was used tentatively in Eq. A22 as an estimate of $A$. Coupling Eq. A22 with equations based on Fick's law, permitted $m_{bb}$ and $b_{bb}$ to be highly constrained based on observed data. In the first optimization, ranges for $m_{bb}$ and $b_{bb}$ were determined based on standard deviations of ten determined values from randomly selected initial values. Then, $Vc_{max25}$, $J_{max25}/Vc_{max25}$, $m_{bb}$, and $b_{bb}$ were determined by minimizing RMSE between observed and modeled GPP, where $m_{bb}$ and $b_{bb}$ were re- determined for the range obtained from the first optimization for λE.

Ranges of parameter uncertainty were given by ten determined values from randomly selected initial values, as we found that the ten iterations for the optimization were enough for determining the global optima (Ueyama et al., 2016). We used determined parameters for subsequent analyses only when parameter uncertainty was less than 10% of the absolute value. Thus, uncertainties of the parameters associated with the optimization were less than 10% of the value.

*A3. Flux partitioning for Asian data*

We post-processed the Asian data for all sites using a standard protocol for data quality control, and flux partitioning (Ichii et al., 2017). Quality control was conducted using a spike detection method (Papale et al., 2006). Data that had been collected under calm night conditions were filtered using the friction velocity threshold (Reichstein et al., 2005). GPP was estimated as the

difference between net ecosystem exchange (NEE) and ecosystem respiration (RE). Daytime RE was based on exponential relationships (Lloyd and Taylor, 1994), which were determined for each day using nighttime data with a 29-day moving window. The daily parameters of the exponential relationship were estimated using an ordinary bootstrapping procedure. In the procedure, qualified nighttime NEE were resampled 100 times without a parametric assumption as the sample size within a moving window was held. Then, RE and GPP were determined as a mean of those fluxes estimated using 100 parameters from 100 resampled data subset. This procedure was conducted using a Flux Analysis Tool program version 2 (Ueyama et al., 2012), which is open source software and is freely available from authors web-site (http://atmenv.envi.osakafu-u.ac.jp/staff/ueyama/softwares/).

**References**


Alberto, M. C. R., Wassmann, R., Hirano, T., Miyata, A., Kumar, A., Padre, A., & Amante, M. (2009) $CO_2$/heat fluxes in rice fields: Comparative assessment of flooded and non-flooded fields in the Philippines. *Agric. For. Meteorol.* **149**, 1737-1750.

Anthoni, P. M., Knohl, A., Rebmann, C., Freibauer, A., Mund, M., Ziegler, W., Kolle, O. & Schulze, E. –D. (2004) Forest and agricultural land-use-dependent $CO_2$ exchange in Thuringia, Germany. *Glob. Change Biol.* **10**, 2005–2019.

Ardö, J., Mölder, M., El-Tahir, B. A., Abdalla, H., & Elkhidir, M. (2008) Seasonal variation of carbon fluxes in a sparse savanna in semi arid Sudan. *Carbon Balance and Management* 3:7.

Baldocchi, D. D., Chen, Q., Chen, X. Ma, S., Miller, G., Ryu, Y., Xiao, J., Wenk, R. & Battles, J. (2010) The dynamics of energy, water, and carbon fluxes in a blue oak (*Quercus douglasii*) savanna in California. *Ecosys. Func. Savannas* **132**, 135-151.

Ball, J., Woodrow, I. & Berry, J., A. (1987) *Progress in Photosynthesis Research*, Martinus Nijho Publishers.

Belelli Marchesini, L. (2007) *Analysis of the carbon balance of steppe and old field ecosystems of Central Asia*. PhD thesis, 209pp, University of Tuscia, Viterbo, Italy, http://dspace.unitus.it/handle/2067/540.

Belelli Marchesini, L., Papale, D., Reichstein, M., Vuichard, N., Tchebakova, N. & Valentini, R. (2007) Carbon balance assessment of a natural steppe of southern Siberia by multiple constraint approach. *Biogeosciences* **4**, 581-595.

Berbigier, P., Bonnefond, J. M. & Mellmann, P. (2001) $CO_2$ and water vapour fluxes for 2 years above Euroflux forest site. *Agric. For. Meteorol.* **108**, 183–197.

Bernacchi, C. J., Pimentel, C. & Long, S. P. (2003) *In vivo* temperature response functions of parameters required to model RuBP-limited photosynthesis. *Plant, Cell Environ*. **26**, 1419-1430.

Bernacchi, C. J., Singsaas, E. L., Pimentel, C., Portis Jr, A. R. & Long, S.P. (2001) Improved temperature response functions for models of Rubisco-limited photosynthesis. *Plant, Cell Environ.* **24**, 253-259.

Bonal, D. et al. (2008) Impact of severe dry season on net ecosystem exchange in the Neotropical rainforest of French Guiana. *Glob. Change Biol.* **14**, 1917-1933.

Carrara, A., Kowalski, A. S., Neirynck, J. & Janssens, I. A. (2003) Net ecosystem $CO_2$ exchange of mixed forest in Belgium over 5 years. *Agric. For. Meteorol.* **119**, 209–227.

Cescatti, A. & Marcolla, B. (2004) Drag coefficient and turbulence intensity in conifer canopies. *Agric. For. Meteorol.* **121**, 197–206.

Chiesa, M., Maselli, F., Bindi, M., Fibbi, L., Cherubini, P., Arlotta, E., Tirone, G., Matteucci, G. & Seufert, G. (2005) Modelling carbon budget of Mediterranean forests using ground and remote sensing measurements. *Agric. For. Meteorol.* **135**, 22–34.

Collatz, G. J., Ball, J. T., Grivet, C. & Berry, J. A. (1991) Physiological and environmental regulation of stomatal conductance, photosynthesis and transpiration: a model that includes a laminar boundary layer. *Agric. For. Meteorol.* **5**, 107-136.

Cook, B. et al. (2004) Carbon exchange and venting anomalies in an upland deciduous forest in northern Wisconsin, USA. *Agric. For. Meteorol.* **126**, 271–295.

Corradi, C., Kolle, O., Walter, K., Zimov, S. A. & Schulze, E. D. (2005) Carbon dioxide and methane exchange of a north-east Siberian tussock tundra. *Glob. Change Biol.* **11**, 1910-1925.

de Pury, D. G. G. & Farquhar, G. D. (1997) Simple scaling of photosynthesis from leaves to canopies without the errors of big-leaf models. *Plant, Cell Environ.* **20**, 537-557.

Desai, A. R., Bolstad, P. V., Cook, B. D.., Davis, K. J. & Carey, E. V. (2005) Comparing net ecosystem exchange of carbon dioxide between an old-growth and mature forest in the upper Midwest, USA. *Agric. For. Meteorol.* **1-2**, 33–55.

Dolman, A. J., Moors, E. J. & Elbers, J. A. (2002) The carbon uptake of a mid latitude pine forest growing on sandy soil. *Agric. For. Meteorol.* **111**, 157–170.

Duan, Q. Y., Gupta, V. K. & Sorooshian, S. (1993) Shuffled complex evolution approach for effective and efficient global minimization. *J. Optim. Theor. Appl.* **76**, 501-521.

Duan, Q. Y., Sorooshian, S. & Gupta, V. K. (1992) Effective and efficient global optimization for conceptual rainfall-runoff models. *Water Resour. Res.* **28**, 1015-1031.

Duan, Q. Y., Sorooshian, S. & Gupta, V. K. (1994) Optimal use of the SCE-UA global optimization method for calibrating watershed models. *J. Hydrol.* **158**, 265-284.

Dunn, A., Barford, C. C., Wofsy, S. C., Goulden, M. L. & Daube, B. C. (2006) A long-term record of carbon exchange in a boreal black spruce forest: means, responses to interannual variability, and decadal trends. *Glob. Change Biol.* **12**, 1–14.

Euskirchen, E. S., Edgar, C. W., Bret-Harte, M. S., Kade, A., Zimov, N., Zimov, S. (2017)

Interannual and seasonal patterns of carbon dioxide, water and energy fluxes from ecotonal and thermokarst-impacted ecosystems on carbon-rich permafrost soils in northeastern Siberia. J *Geophys Res Biogeosci* **122**, 51-2668. doi:10.1002/2017JG004070.

Farquhar, G. D., von Caemmerer, S. & Berry, J. A. (1980) A biochemical model of photosynthesis $CO_2$ assimilation in leavers of C3 species. *Planta* **149**, 78-90.

Frank, D. C. et al. (2015) Water-use efficiency and transpiration across European forests during the Anthropocene. *Nature Clim. Change* **5**, 579-583.

Gamo, M., Panuthai, S., Maeda, T., Toma, T., Ishida, A., Hayashi, M., Warsudi, D. R., Diloksumpun, S., Phanumard, L., Staporn, D., Ishizuka, M., Saigusa, N. & Kondo, H. (2005) Carbon flux observation in the tropical seasonal forests and tropical rain forest. *Proceedings of the International Workshop on Advanced Flux Network and Flux Evaluation (AsiaFlux Workshop 2005)*, Fujiyoshida, Japan, 86 pp.

Garbulsky, M. F., Penuelas, J., Papale, D. & Filella, I. (2008) Remote estimation of carbon dioxide uptake by a Mediterranean forest. *Glob. Change Biol*. **14**, 2860–2867.

Gough, C. et al. Sustained carbon uptake and storage following moderate disturbance in a Great Lake forest. *Ecol. Appl*. **23**, 1202-1215.

Goulden, M., Miller, S. D., & de Rocha, H. (2006) Nocturnal cold air drainage and pooling in a tropical forest. *J. Geophys. Res.* **111**, D08S04, doi:10.1029/2005JD006037.

Grünwald, T., Berhofer, C. (2007) A decade of carbon, water and energy flux measurements of an old spruce forest at the Anchor Station Tharandt. *Tellus* **59B**, 387-396.

Harazono, Y., Li, S., Shen, J. & He, Z. (1993) Seasonal micrometeorological changes over a grassland in Inner Mongolia. *J. Agric. Meteorol*. **48**, 711-714.

Harazono, Y., Yoshimoto, M. & Kawamura, T. (1996) Photosynthesis rate distribution and light use efficiency within a soybean canopy determined by numerical simulation with the neo soil-plant-atmosphere model. *J. Agric. Meteorol*. **52**, 281-291 (*in Japanese with English abstract*).

He, L., Chen, J. M., Pisek, J., Schaaf, C. B. & Strahler, A. H. (2012) Global clumping index map derived from the MODIS BRDF product. *Remote Sens. Environ.* **119** 118-130.

Hirano, T., Segah, H., Harada, T., Limin, S., June, T., Hirata, R., & Osaki, M. (2007) Carbon dioxide balance of a tropical peat swamp forest in Kalimantan, Indonesia. *Glob. Change Biol.* **13**, 412–425.

Hirano, T., Segah, H., Kusin, K., Limin, S., Takahashi, H. & Osaki, M. (2012) Effects of disturbances on the carbon balance of tropical peat swamp forests. *Glob. Change Biol.* **18**, 3410-3422.

Hirata, R., Hirano, T., Saigusa, N., Fujinuma, Y., Inukai, K., Kitamori, Y., Takahashi, Y. & Yamamoto, S. (2007) Seasonal and interannual variations in carbon dioxide exchange of a temperate larch forest. *Agric. Forest Meteorol*. **147**, 110–124.

Hutley, L. B., Leuning, R., Beringer, J. & Cleugh, H. A. (2005) The utility of the eddy covariance techniques as a tool in carbon accounting: tropical savanna as a case study. *Australian J. Botany* **53**, 663-675.

Hsieh, C.-I., Lai, M.-C., Hsia, Y.-J. & Chang, T.-J. (2008) Estimation of sensible heat, water vapor, and $CO_2$ fluxes using the flux-variance method. *Int. J. Biometeorol*. **52**, 521-533.

Ichii, K. et al. (2017) New data-driven estimation of terrestrial $CO_2$ fluxes in Asia using a standardized database of eddy covariance measurements, remote sensing data, and support vector regression. *J. Goephys. Res. Biogeosciences* **122**, 767-795.

Kato, T., Tang, Y., Gu, S., Hirota, M., Du, M., Li, Y. & Zhao, X. (2006) Temperature and biomass influences on interannual changes in $CO_2$ exchange in an alpine meadow on the Qinghai-Tibetan Plateau. *Glob. Change Biol*. **12**, 1285–1298.

Kattge, J. & Knorr, W. (2007) Temperature acclimation in a biochemical model of photosynthesis: a reanalysis of data from 36 species. *Plant, Cell Environ.* **30**, 1176-1190.

Kitamura, K., Nakai, Y., Suzuki, S., Ohtani, Y., Yamanoi, K. & Sakamoto, T. (2012) Interannual variability of net ecosystem production for a broadleaf deciduous forest in Sapporo, northern Japan. *J. Forest Res.* **17**, 323-332.

Knauer, J. et al. (2018) Towards physiologically meaningful water-use efficiency estimates from eddy covariance data. *Global Change Biol*. **24**, 694-710.

Knohl, A. & Buchmann, N. (2005) Partitioning the net $CO_2$ flux of a deciduous forest into respiration and assimilation using stable carbon isotopes. *Glob. Biogeochem. Cycles* **19**. GB4008.

Kosugi, Y., Shibata, S. & Kobashi, S. (2003) Parameterization of the $CO_2$ and $H_2O$ gas exchange of several temperate deciduous broad-leaved trees at the leaf scale considering seasonal changes. *Plant, Cell Environ.* **26**, 285-301.

Kosugi, Y., Takanashi, S., Ueyama, M., Ohkubo, S., Tanaka, H., Matsumoto, K., Yoshifuji, N., Ataka, M. & Sakabe, A. (2013) Determination of the gas exchange phenology in an evergreen coniferous forest from 7 years of eddy covariance flux data using an extended big-leaf analysis. *Ecol. Res*. **28**, 373-385.

Kosugi, Y., Tanaka, H., Takanashi, S., Matsuo, N., Ohte, N., Shibata, S. & Tani, M. (2005) Three years of carbon and energy fluxes from Japanese evergreen broad-leaved forest. *Agric. For. Meteorol.* **132**, 329-343.

Kosugi, Y., Takanashi, S., Ohkubo, S., Matsuo, N., Tani, M., Mitani, T., Tsutsumi, D., & Nik, A. R. (2008) $CO_2$ exchange of a tropical rainforest at Pasoh in Peninsular Malaysia. *Agric. For. Meteorol.* **148**, 439-452.

Kumagai, T., Ichie, T., Yoshimura, M., Yamashita, M., Tanaka, K., Saitoh, T. M., Ohashi, M., Suzuki, M., Koike, T. & Komatsu, H. (2006) Modeling $CO_2$ exchange over a Bornean tropical

rain forest using measured vertical and horizontal variations in leaf-level physiological parameters and leaf area densities. *J. Geophys. Res.* **111**, D10107, doi:10.1029/2005JD006676.

Kutsch, W. L., Hanan, N., Scholes, B., McHugh, I., Kubheka, W., Eckhardt, H. & Williams, C. (2008) Response of carbon fluxes to water relations in a savanna ecosystem in South Africa. *Biogeosciences* **5**, 1797-1808.

Kwon, H., Kim, J., Hong, J. & Lim, J. H. (2010) Influence of the Asian monsoon on net ecosystem carbon exchange in two major ecosystems in Korea. *Biogeosciences*, **7**, 1493-1504.

Kwon, H., Park, T., Hong, J., Lim, J. & Kim, J. (2009) Seasonality of net ecosystem carbon exchange in two major plant functional types in Korea. *Asia-Pacific J. Atmos. Sci.* **45**, 149–163.

Leuning, R., Cleugh, H. A., Zegelin, S. J. & Hughes, D. (2005) Carbon and water fluxes over a temperate *Eucalyptus* forest and a tropical wet/dry savanna in Australia: measurements and comparison with MODIS remote sensing estimates. *Agric. For. Meteorol*. **129**, 151–173.

Lhomme, J. P., Chehbouni, A. & Monteny, B. (2000) Sensible heat flux-radiometric surface temperature relationship over sparse vegetation: parameterizing B-1. *Boundary-Layer Meteorol.* **97**, 431-457.

Li, S.-G., Asanuma, J., Eugster, W., Kotani, A., Davaa, G., Oyunbaatar, D. & Sugita, M. (2005a) Net ecosystem carbon dioxide exchange over grazed steppe in central Mongolia. *Glob. Change Biol.* **11**, 1941–1955.

Li, S.-G., Asanuma, J., Kotani, A., Eugster, W., Davaa, G., Oyunbaatar, D. & Sugita, M. (2005b) Year-round measurements of net ecosystem $CO_2$ flux over a montane larch forest in Mongolia. *J. Geophys. Res.* **110**, D09303, doi:10.1029/2004JD005453.

Lloyd, J., Taylor, J. A. (1994) On the temperature dependence on soil respiration. *Funct. Ecol.* **8**, 315-323.

Lloyd, J. et al. (2010) Optimization of photosynthetic carbon gain and within-canopy gradients of associated foliar traits for Amazon forest trees. *Biogeosciences* **7**, 1833-1859.

Ma, S., Baldocchi, D. D., Xu, L., Hehn, T. (2007) Inter-annual variability in carbon dioxide exchange of an oak/grass savanna and open grassland in California. *Agric. For. Meteorol*. **147**, 157–171.

Machimura, T., Kobayashi, Y., Iwahana, G., Hirano, T., Lopez, L., Fukuda, M. & Fedorov, A. N. (2005) Change of carbon dioxide budget during three years after deforestation in eastern Siberian larch forest. *J. Agric. Meteorol.* **60**, 653-656.

Marcolla, B. & Cescatti, A. (2005) Experimental analysis of flux footprint for varying stability conditions in an alpine meadow. *Agric. For. Meteorol*. **135**, 291–301.

Marushchak, M. E., Kiepe, I., Biasi, C., Elsakov, V., Friborg, T., Johansson, T., Soegaard, H., Virtanen, T. & Martikainen, P. J. (2013) Carbon dioxide balance of subarctic tundra from plot

to regional scales. *Biogeosciences* **10**, 437-452.

Matsumoto, K., Ohta, T., Nakai, T., Kuwada, T., Daikoku, K., Iida, S., Yabuki, H., Kononov, A. V., van der Molen, M. K., Kodama, Y., Maximov, T. C., Dolman, A. J. & Hattori, S. (2008) Responses of surface conductance to forest environments in the Far East. *Agric. For. Meteorol*. **148**, 1926–1940.

Merbold, L., et al. (2009) Precipitation as driver of carbon fluxes in 11 African ecosystems. *Biogeosciences* **6**, 1027-1041.

Merbold, L., Kutsch, W. L., Corradi, C., Kolle, O., Rebmann, C., Stoy, P. C., Zimov, Z. A. & Schulze, E.-D. (2009) Artificial drainage and associated carbon fluxes ($CO_2$/$CH_4$) in a tundra ecosystem. *Glob. Change Biol.* **15**, 2599-2614.

Milyukova, I., Kolle, O. Varlagin, A., Vygodskaya, N., Schulze, E. & Lloyd, J. (2002) Carbon balance of a southern taiga spruce stand in European Russia. *Tellus B* **54**, 429-442.

Miyata, A., Harazono, Y., Shen, J. & Li, S. (1993) Turbulent transfer of momentum, water vapor and carbon dioxide over a due and a glassland in Inner Mongolia. *J. Agric. Meteorol*. **48**, 715-718.

Mizoguchi, Y., Ohtani, Y., Takanashi, S., Iwata, H., Yasuda, Y. & Nakai, Y. (2012) Seasonal and interannual variation in net ecosystem production of an evergreen needle leaf forest in Japan. *J. For. Res.* **17**, 283–295.

Montagnani, L. et al. (2009) A new mass conservation approach to the study $CO_2$ advection in an alpine forest. *J. Geophys. Res.: Atm.* **114**, D07306, doi:10.1029/2008JD010650.

Monteith, J. L. (1965) Evaporation and environment. *Symp. Soc. Exp. Biol*. **19**, 205-224.

Moureaux, C., Debacq, A., Bodson, B., Heinesch, B. & Aubinet, M. (2006) Annual net ecosystem carbon exchange by a sugar beet crop. *Agric. For. Meteorol.* **139**, 25–39.

Nakai, Y., Matsuura, Y., Kajimoto, T., Abaimov, A. P., Yamamoto, S., & Zyryanova, O. A. (2008) Eddy covariance $CO_2$ flux above a Gmelin larch forest on continuous permafrost of central Siberia during a growing season. *Theor. Appl. Climatol.* **93**, 133–147.

Norby, R. J. et al. (2005) Forest response to elevated $CO_2$ is conserved across a broad range of productivity. *Proc. Natl. Acad. Sci. USA* **102**, 18925-18930.

Oliphant, A. J. et al. (2004) Heat storage and energy balance fluxes for a temperate deciduous forest. *Agric. For. Meteorol.* **126**, 185–201.

Papale, D., et al. (2006) Towards a standardized processing of net ecosystem exchange measured with eddy covariance technique: algorithms and uncertainty estimation. *Biogeosciences* **3**, 571-583.

Pilegaard, K., Hummelshøj, P., Jensen, N. O. & Chen, Z. (2001) Two years of continuous $CO_2$ eddy-flux measurements over a Danish beech forest. *Agric. For. Meteorol.* **107**, 29–41.

Pisek, J. et al. (2015) Intercomparison of clumping index estimates from POLDER, MODIS, and

MISR satellite data over reference sites. *ISPRS J. Photo. Remote Sens*. **101** 47-56.

Posse, G., Lewxzuk, N., Richter, K. & Cristiano, P. (2016) Carbon and water vapor balance in a subtropical pine plantation. *iForest* doi: 10.3832/ifor1815-009.

Prescher, A.-K., Grünwald, T. & Berhofer, C. (2010) Land use regulates carbon budgets in eastern Germany: From NEE to NBP. *Agric. For. Meteorol.* **150**, 1016–1025.

Rambal, S., Joffre, R., Ourcival, J. M., Cavender-Bares, J. & Rocheteau, A. (2004) The growth respiration component in eddy $CO_2$ flux from a *Quercus ilex* mediterranean forest. *Glob. Change Biol.* **10**, 1460-1469.

Reichstein, M. et al. (2005) On the separation of net ecosystem exchange into assimilation and ecosystem respiration: review and improved algorithm. *Glob. Change Biol.* **11**, 1-16.

Rinne, J. et al. (2000) Measurements of hydrocarbon fluxes by a gradient method above a norther boreal forest. *Agric. For. Meteorol.* **102**, 25–37.

Ross, J. (1981) The radiation regime and architecture of plant stands. Junk Publishers, The Hague, 391 pp.

Ryu, Y., et al. (2011) Integration of MODIS land and atmosphere products with a coupled-process model to estimate gross primary productivity and evapotranspiration from 1 km to global scales. *Glob. Biogeochem. Cycles* **25**, doi:10.1029/2011GB004053.

Saigusa, N., Yamamoto, S., Murayama, S. & Kondo, H. (2005) Interannual variability of carbon budget components in an AsiaFlux forest site estimated by long-term flux measurements. *Agric. For. Meteorol.* **134**, 4–16.

Saito, M., Miyata, A. Nagai, H. & Yamada, T. (2005) Seasonal variation of carbon dioxide exchange in rice paddy field in Japan. *Agric. For. Meteorol*. **135**, 93–109.

Saitoh, T. M., Tamagawa, I., Muraoka, H., Lee, N.-Y., Yashiro, Y. & Koizumi, H. (2010) Carbon dioxide exchange in a cool-temperate evergreen coniferous forest over complex topography in Japan during two years with contrasting climates. *J. Plant Res*. **123**, 473–483.

Sakuratani, T. & Horie, T. (1985) Studies on evapotranspiration from crops (1) On seasonal changes, vertical differences and the simplified methods of estimate in evapotranspiration of paddy rice. *J. Agr. Meteorol*. **41**, 45-55 in Japanese.

Scartazza, A., Mata, C., Matteucci, G., Yakir, D., Moscatello, S. & Brugnoli, E. (2004) Comparisons of $\delta^{13}C$ of photosynthetic products and ecosystem respiratory $CO_2$ and their responses to seasonal climate. *Oecologica* **140**, 340-31.

Scott, R. L., Hamerlynck, E. P., Jenerette, G. D., Moran, M. S. & Barron-Gafford, G. A. (2010) Carbon dioxide exchange in a semidesert grassland through drought-induced vegetation change. *J. Geophys. Res.: Biogeosciences* **115**, G03026, doi:10.1029/2010JG001348.

Scott, R. L., Jenerette, G. D., Potts, D. L., Huxman, T. E. (2009) Effects of seasonal drought on net carbon dioxide exchange from a woody-plant-encroached semiarid grassland. *J. Geophys.*

*Res.: Biogeosciences* **114**, G04004, doi:10.1029/2008JG000900.

Shimizu, T., Suzuki, M. & Shimizu, A. (1999) Examination of a Correction Procedure for the Flow Attenuation in Orthogonal Sonic Anemometers. *Boundary-Layer Meteorol*. **93**, 227-236.

Sprintsin, M., Cohen, S., Maseyk, K., Rotenberg, E., Grünzweig, J., Karnieli, A., Berliner, P. & Yakir, D. (2011) Long term and seasonal courses of leaf area index in a semi-arid forest plantation. *Agric. For. Meteorol*. **151**, 565-574.

Su, H. B., Paw U, K. T. & Shaw, R. H. (1996) Development of a coupled leaf and canopy model for the simulation of plant-atmosphere interaction. *J. Appl. Meteorol*. **35**, 733-748.

Sulman, B. N., Desai, A. R., Cook, B. D., Saliendra, N. & Mackay, D. S. (2009) Contrasting carbon dioxide fluxes between a drying shrub wetland in northern Wisconsin, USA, and nearby forests. *Biogeosciences* **6**, 1115-1126.

Sun, O., Campbell, J., Law, B. E. & Wolf, V. (2004) Dynamics of carbon stocks in soils and detritus cross chronosequences of different forest types in the Pacific Northwest, USA. *Glob. Change Biol.* **10**, 1470-1481.

Takagi, K., Fukuzawa, K., Liang, N., Kayama, M., Nomura, M., Hojyo, H., Takahashi, Y., Nakaji, T., Oguma, H. & Fujinuma, Y. (2009) Change in $CO_2$ balance under a series of forestry activities in a cool-temperate mixed forest with dense undergrowth. *Global Change Biol*. **15**, 1275–1288.

Takagi, K., Miyata, A., Harazono, Y., Ota, N., Komine, M. & Yoshimoto, M. (2003) An alternative approach to determining zero-plane displacement, and its application to a lotus paddy field. *Agric. For. Meteorol*. **115**, 173-181.

Takahashi, Y., Saigusa, N., Hirata, R., Ide, R., Fujinuma, Y., Okano, T. & Arase, T. (2015) Characteristics of temporal variations in ecosystem $CO_2$ exchange in a temperate deciduous needle-leaf forest in the foothills of a high mountain. *J. Agric. Meteorol*. **71**, 302-317.

Tan, Z.-H., Zhang, Y.-P., Schaefer, D., Yu, G.-R., Liang, N. & Song, Q.-H. (2011) An old-growth subtropical Asian evergreen forest as a large carbon sink. *Atmos. Environ.* **48**, 1548–1554.

Tanja, S., et al. (2003) Air temperature triggers the recovery of evergreen boreal forest photosynthesis in spring. *Glob. Change Biol.* **9**, 1410-1426.

Ueyama, M., Hirata, R., Mano, M., Hamotani, K., Harazono, Y., Hirano, T., Miyata, A., Takagi, K., Takahashi, Y. (2012) Influences of various calculation options on heat, water, and carbon fluxes determined by open- and closed-path eddy covariance method. *Tellus B* **64**, 19048.

Ueyama, M. et al. (2016) Optimization of biochemical model with eddy covariance measurements in black spruce forests of Alaska for estimating $CO_2$ fertilization effects. *Agric For. Meteorol.* **222**, 98-111.

Ulke, A. G., Gattinoni, N. N. & Posse, G. (2015) Analysis and modelling of turbulent fluxes in two different ecosystems in Argentina. *Int. J. Environ. Pollut*. **58**, 52-62.

Urbanski, S. et al. (2007) Factors controlling $CO_2$ exchange on timescales from hourly to decadal at Harvard Forest. *J. Geophys. Res.: Biogeosciences* **112**, G2020, doi:10.1029/2006JG000293.

van Huissteden, J., Maximov, T. C. & Dolman, A. J. (2005) High methane flux from an arctic floodplain (Indigirka lowlands, eastern Siberia), *J. Geophys. Res.: Biogeosciences* **110**, G02002, doi:10.1029/2005JG000010.

von Caemmerer, S., Farquhar, G. & Berry, J. (2009) Biochemical model of C3 photosynthesis. In: Photosynthesis in silico: Understanding Complexity from Molecules to Ecosystems (ed. Laisk A, Nedbal L, Govindjee), pp. 209-230. Springer, USA.

Wang, H., Saigusa, N., Zu, Y., Yamamoto, S., Kondo, H., Yang, F., Wang, W., Hirano, T. & Fujinuma, Y. (2005) Response of $CO_2$ flux to environmental variables in two larch forest ecosystems in East Asia. *Phyton* **45**, 339–346.

Wang, L.. Stephen, P. G. & Caylor, K. K. (2014) Global synthesis of vegetation control on evapotranspiration partitioning. *Geophys. Res. Lett*. **41**, 6753-6757.

Wang, Y. P., Baldocchi, D., Leuning, R., Falge, E. & Vesala, T. (2007) Estimating parameters in a land-surface model by applying nonlinear inversion to eddy covariance flux measurements from eight FLUXNET sites. *Glob. Change Biol.* **13**, 652-670.

Weiss, A. & Norman, J. M. (1985) Partitioning solar radiation into direct and diffuse, visible and near-infrared components. *Agric. For. Meteorol*. **34**, 205-213.

Wenzel, S., Cox, P. M., Eyring, V. & Friedlingstein, P. (2016) Projected land photosynthesis constrained by changes in the seasonal cycle of atmospheric $CO_2$. *Nature* **538**, 499-501.

Wohlfahrt, G., Hammerle, A., Haslwanter, A., Bahn, M., Tappeiner, U. & Cernusca, A. (2008)S easnal and inter-annual variability of the net ecosystem $CO_2$ exchange of a temperate mountain grassland: Effects of weather and management. *J. Geophys. Res.: Biogeosciences* **113**, D08110, doi:10.1029/2007JG009286.

Wullschleger, S. D., (1993) Biochemical limitations to carbon assimilation in $C_3$ plants-a retrospective analysis of the $A/C_i$ curves 109 species. *J. Exp. Bot.* **44**, 907-920.

Yasuda, Y., Saito, T., Hoshino, D., Ono, K., Ohtani, Y., Mizoguchi, Y., & Morisawa, T. (2012) Carbon balance in a cool–temperate deciduous forest in northern Japan: seasonal and interannual variations, and environmental controls of its annual balance. *J. For. Res.* **17**, 253-267.

Yasuda, Y., & Watanabe, T. (2001) Comparative measurements of $CO_2$ flux over a forest using closed-path and open-path $CO_2$ analyzers. *Boundary-Layer Meteorol*. **100**, 191-208.

Yu, G.-R., Wen, X.-F., Sun, X.-M., Tanner, B. D., Lee, X. & Chen, J.-Y. (2006) Overview of ChinaFLUX and evaluation of its eddy covariance measurement. *Agric. Forest Meteorol.* **137**, 125–137.

Yu, G.-R., Zhang, L.-M., Sun, X.-M., Fu, Y.-L., Wen, X.-F., Wang, Q.-F., Li, S.-G., Ren, C.-Y.,

Song, X., Liu, Y.-F., Han, S.-J. & Yan J.-H. (2008) Environmental controls over carbon exchange of three forest ecosystems in eastern China. *Glob. Change Biol.* **14**, 2555–2571.

Zeeman, M. J., Hiller, R., Gilgen, A. K., Michna, P., Plüss, P., Buchmann, N. & Eugster, W. (2010) Management and climate impacts on net $CO_2$ fluxes and carbon budgets of three grasslands along an elevation gradient in Switzerland. *Agric For. Meteorol.* **150**, 519-530.

Zweifel, R., Eugster, W., Etzold, S., Dobbertin, M., Buchmann, N. & Häsler, R. (2010) Link between continuous stem radius changes and net ecosystem productivity of a subalpine Norway spruce forest in the Swiss Alps. *New Phytologist* **187**, 819-830.